

GBT Pointing Coefficient Estimates
For Phase I,
From Metrology Measurements.

Michael A. Goldman, Dana S. Balser, Don Wells

March 18, 1999

Abstract

Metrology measurements have been proposed to provide initial estimated pointing coefficients for the Green Bank Telescope (GBT) before astronomical observations can be made. The measurements are made by laser ranging from ground-based rangefinders to targets on the antenna structure, using 2-axis tiltmeters on the alidade and tipping structures, and a hydrostatic leveling system on the azimuth track. Algorithms and equations are given for the conversion of metrology data into pointing coefficients. The pointing coefficients include contributions to correct for deflection of the GBT local gravity vertical from the geodetic zenith.

0.1. Introduction

Pointing of the Green Bank Telescope will be guided by the azimuth and elevation pointing series described by Condon [Con 92]. If a reasonable initial set of estimates for most of the pointing coefficients appearing in these series is provided before astronomical measurements are made, then in principle valuable time can be saved during GBT commissioning.

A measurement program was proposed by Hall et al. [HGPP 98] to characterize the GBT by metrology methods. These include laser ranging, tiltmeters, accelerometers, and other instrumental techniques. As part of this program, measurements would be made to provide a-priori estimates for most of the coefficients defined in [Con 92]. A description of the proposed program, schedule, and measurements is given in a draft memo [PG 98].

Earlier documents have appeared which discuss the use of metrology methods to obtain pointing coefficients: [Gol 97], [Wel 98], [PG 98]. The present memo reviews and extends those discussions, and gives detailed analysis to process measurement data to provide pointing coefficients. In particular we analyze contributions to the pointing series coefficients which are due to tilt of the azimuth track and collimation of the elevation axis, that is departure from perpendicularity of the elevation and azimuth axes of the telescope. We define and measure four parameters which describe the track tilt and elevation axis collimation and analytically derive the expected pointing series coefficient contributions to be expected in terms of these parameters. We also discuss corrections to be expected due to the deflection of the local gravity vertical from local geodetic zenith.

A major goal is to use available metrology tools to isolate specific defects in the telescope structure. This is accomplished by measuring the telescope structure and using the results of each measurement to decouple defects which collectively are represented by single terms in the traditional pointing model. We begin by using the hydrostatic leveling system to measure the azimuth track (see [Pel 92; Pel 93] for information about the Pellissier Model H5 hydrostatic level and [MR 98] for a description of the Green Bank system). These measurements will be able to determine the average tilt of the azimuth track independent of the alidade or

tipping structure. Next, two 2-axis tiltmeters placed below the elevation bearings on the alidade will provide a model of the azimuth track. Unlike hydrostatic level results, defects in the alidade structure, including problems in the wheels, etc. should be present in the data. Then, if necessary, additional measurements can be designed and made subsequently, based on the results. Last, laser rangefinder measurements from the ground to targets on the alidade, box structure, and feed arm will measure the elevation axis collimation (see [Par 97] for a comprehensive review of the GBT laser metrology project). Defects in the azimuth track and alidade will necessarily be included in the analysis of the laser rangefinder data.

Pointing coefficients expected to be important for the GBT are reproduced from [Wel 98], and appear in Table 1. (A typographical error in [Wel 98] Table 1 has been corrected: $a_{1,1}^{AZ}$ and $b_{1,1}^{AZ}$ were interchanged; the source code is correct, however.) The double subscript notation is that which appears in the GBT's monitor and control system source code software.

In this memo we assume the following convention: The azimuth and elevation variables A and E which appear in the pointing series are *geodetic* azimuth and elevation respectively of the radio object to be observed at a given local apparent sidereal time. Correction terms ΔA and ΔE are computed using the pointing series. The angles $A + \Delta A$ and $E + \Delta E$ are then the commanded beam position azimuth and elevation angles respectively for the telescope drive system. The telescope is driven so that the encoder output angle readings are equal to the respective commanded angles at the specified time of observation.

Table 1: A Comparison Of Pointing Formula Notations.

$\Delta A \cos E$ (Azimuth Pointing Series Terms)								
Condon Series()								
Coeff	Term	Meaning	Con92	vH93	Stu72	Mur92	Cla74 ^a	Nei96 ^b
$d_{0,0}$	1	Hor. Col.	C_1	P_5	P_1	C_9	A_6	P_1^c
$b_{0,1}$	$\sin E$	El. Ax. Col.	C_3	P_3	P_3	C_8	A_5	P_3
$d_{0,1}$	$\cos E$	Az Zero	C_2	P_6	P_2	C_5	A_7	P_2
$b_{1,1}$	$\cos A \sin E$	Zen E -Tilt	C_4	P_2	P_4	C_6	A_1	P_4
$a_{1,1}$	$\sin A \sin E$	Zen N -Tilt	C_5	P_1	P_5	C_7	A_2	P_5
$c_{2,1}$	$\sin 2A \cos E$	Az Track						
$d_{2,1}$	$\cos 2A \cos E$	Az Track						

ΔE (Elevation Pointing Series Terms)								
Condon Series()								
Coeff	Term	Meaning	Con92	vH93	Stu72	Mur92	Cla74	Nei96
$d_{0,0}$	1	Elev Zero	C_6	P_4	P_7	C_1	D_5	P_7^c
$c_{1,0}$	$\sin A$	Zen E -Tilt	C_4	P_2	P_4	C_3	D_1	P_4
$d_{1,0}$	$\cos A$	Zen N -Tilt	C_5	P_1	P_5	C_2	D_2	P_5
$b_{0,1}$	$\sin E$	Asym Gravity		P_8			D_4	"G"
$d_{0,1}$	$\cos E$	Symm Gravity	C_7	P_7	P_8	C_4	D_3	P_8

^a The VLA formula for $\Delta A \cos E$ includes terms $A_3 \cos A \cos E$ and $A_4 \sin A \cos E$ which correspond to inactive GBT terms $d_{1,1}^{(AZ)}$ and $c_{1,1}^{(AZ)}$. These terms represent “azimuth encoder centering error” and are of period one turn. The analogous terms in elevation have the same form as the two gravity bending terms.

Some VLA antennas are known to exhibit significant $3A$ terms in their pointing (VLA antennas have *three* azimuthal support points), but these are not implemented in the VLA pointing formulae because high frequency operations are now done by frequent reference source offsets; that procedure automatically corrects for those terms [Ken Sowinsky, private communication].

^b Neidhöfer [Nei 96] includes Stumpff’s P_6 terms in the current Effelsberg 100-meter telescope implementation of $\Delta A \cos E$ and ΔE with amplitude of order $\pm 10 \mu$ -radians. (See. discussion in section 6 of [Wel 98].)

^c Neidhöfer [Nei 96] calls this term P_{10} and gives a formula for it which includes P_1 plus terms for daily empirical zero-point-corrections, receiver offset, and polarization effects. He gives analogous formulae for P_2 and P_7 . He states that these are the formulae which are implemented on the Max Planck Institute 100 meter instrument.

0.2. Metrology Equipment

The following resources and data should be available to carry out the proposed pointing coefficient measurements:

- At least seven operational and calibrated ground-based laser rangefinders. It is expected that twelve rangefinders will be available at the time of measurement. Functioning temperature, pressure and humidity instrumentation to correct range data for atmospheric refraction must be available.
- High accuracy 2-axis tiltmeters. These instruments are placed on the alidade structure, near each end of the elevation axle.
- A water level measuring system which can measure over distances of 60 meters. This system has had extensive development at NRAO Green Bank. The water level system provides a way to determine the alidade track elevation profile and mean alidade track plane, independent of the alidade structure. It provides essentially the same information as the tiltmeters, but requires more extensive setup and measurement time.
- Ball retroreflector targets. Two ball targets are mounted under each elevation bearing's weldment platform. Additional targets are mounted under the lower corners of the box structure, at the end of the horizontal feed arm, and on the vertical feed arm.
- Survey control coordinates for the ground-based rangefinders. These must be obtained by an *a-priori* control survey, and a reduction and adjustment of the survey data.
- Ground rangefinder aiming coordinates for the GBT retroreflector targets. These are generated from a data base table of retrotarget reference point coordinates (in the main-reflector or alidade reference frame, as appropriate for the retrotarget referenced to the telescope's 50.8° rigging elevation angle), together with transformation equations to obtain ground rangefinder platform local aiming coordinates as functions of telescope azimuth and elevation. The accuracy required of the coordinates supplied for aiming will generally be significantly less than the accuracy of the range measurements.

- Operational software to reduce rangefinder measured phase to range distance between rangefinder scan reference point and retrotarget fiducial reference point.
- Operational software to adjust range distances for trilateration determinations, to obtain ground coordinates of targets on the telescope.
- A North-South direction survey reference fiducial. This is a survey monument pair defining a horizontal reference line along a near North-South direction. The precise bearing of this reference direction line from astronomical North is measured by surveying its bearing angle from Polaris, and making appropriate ephemeris corrections for the position of Polaris at the time of survey. The detailed procedure is described in [Kav 96]. The ground coordinate system's Y -axis is chosen to be horizontal and directed to local astronomical North, as consistent with the direction of the surveyed reference line. Both geodetic and astronomic azimuths of this line will be specified. The geodetic azimuth of this line is also determined, by making a horizontal Laplace correction [Lei 90].
- Control software to aim the rangefinders to retroreflector targets mounted on the GBT alidade and tipping structures.
- Operating telescope azimuth and elevation encoders, with available encoder readout supplied to the metrology system ZIY-computer.
- Functioning analytical code software to data base the rangefinder and tilt-meter measurement data and to analyze this data to generate pointing coefficients.

0.3. Metrology Measurements And Analysis

0.3.1. Hydrostatic level measurements of the azimuth track

Level measurements of the azimuth track will be made by the Green Bank hydrostatic level to define the mean plane in which the GBT moves in azimuth. The normal to this plane is the zenith vector, \widehat{W} , of the GBT which can deviate from the local vertical. By measuring the deviation of the telescope zenith from vertical, one can obtain an *a-priori* pointing correction due to alidade track tilt. Tilt of the mean alidade track plane is measured directly, independent of the alidade structure, by this method.

Fig. 1 shows the geometry. Unit orthogonal basis vectors \widehat{X} , \widehat{Y} , \widehat{Z} define a fixed ground-based reference frame for describing the telescope geometry. A ground based Cartesian X, Y, Z coordinate system with its axes respectively parallel to those frame vectors has its origin at the intersection point of the telescope azimuth axis at the mean alidade track level. The unit frame basis vector \widehat{Z} is directed along the local upward gravity vertical at the coordinate system origin. The vector \widehat{Y} is directed horizontally along local astronomical North, at the coordinate system origin. The vector \widehat{X} is defined by the relation: $\widehat{X} \equiv \widehat{Y} \times \widehat{Z}$. \widehat{X} is horizontal and points eastward in a positive sense. The telescope's alidade track is initially approximated by a geometric plane, the "Mean Alidade Track Plane.". Unit vector \widehat{W} is the normal to this plane; it is the zenith vector of the GBT. Angle ζ_T is the angle between the zenith vector and gravity vertical. The horizontal bearing of the telescope's zenith vector relative to \widehat{Y} is given by Φ_T . Level measurements of track elevation versus azimuth are used to determine a physical plane which best embodies the Mean Alidade Track Plane, in some least squares sense.

The hydrostatic level data provides a set of track level heights as a function of azimuth, $H = H(AZ)$. It is assumed that astronomical North has been previously measured, and a control network of survey markers has been established so that the ground frame axis directions are known relative to the ground survey control network. The measured heights are relative track elevations along the direction of the local gravity vertical, \widehat{Z} . The heights are measured relative to a fixed bench mark (not loaded) near the GBT center. The height profile data is least-squares-fitted to a sinusoid with an amplitude H_1 and an azimuth Φ_{\min} of minimum height. The pair of angles (ζ_T, Φ_T) are then given by:

$$(3.1.01) \quad \tan(\zeta_T) = \frac{H_1}{R} \quad \text{and}$$

$$(3.1.02) \quad \Phi_T = \Phi_{\min}$$

where R is the radius of the track in the same units as H_1 . Appendix A describes an algorithm which can be used to fit a sine wave.

The design radius of the track center line is: $R = 1260.0$ inches. On 24 October 1992 the track was set and was recorded to be level to ± 0.015 inches. On 23 June 1993 the track was grouted, cured, and 70% rechecked. The level to ± 0.015 " was found to still be true [Mor 97]. A slope of 0.015" per 1260" corresponds to 2.46 arc-seconds angle. It is to be expected *a-priori* that ζ_T will not significantly exceed this tilt, assuming that the track has not significantly deformed or moved since 1993.

Hydrostatic level measurements are too labor and time intensive to be used to provide information on the "fine structure" of the azimuth track. They are however suitable to give an estimate for the track tilt terms in Table 1. These pointing coefficients can be expressed in terms of the azimuth track tilt parameters ζ_T and Φ_T by either using spherical trigonometry or rotation matrices. For example, the tilted track in Fig. 1 can be described as two small rotations about the orthogonal axes X and Y. [Con 92] has derived the coefficients in terms of tilted angles to the north $\Delta N = \zeta_T \cdot \cos(\Phi_T)$ and the west $\Delta W = -\zeta_T \cdot \sin(\Phi_T)$. Using Eq. (5) of [Con 92] yields:

$$(3.1.03) \quad a_{1,1}^{(AZ)} = a_{1,0}^{(EL)} = \zeta_T \cdot \cos(\Phi_T) \quad \text{and}$$

$$(3.1.04) \quad -b_{1,1}^{(AZ)} = c_{1,0}^{(EL)} = \zeta_T \cdot \sin(\Phi_T) .$$

0.3.2. Tiltmeter measurements at the elevation axle

A 2-axis tiltmeter will be placed at each end of the elevation axle, near the bearing (see Fig. 2). Instrument leads will be run to the alidade room and will terminate at a GPIB instrument bus and the readouts sent to a dedicated computer used for the measurement program.

When the telescope moves in azimuth, deviations or bumps in the track can be detected. The readout of each tiltmeter is measured versus the encoder reading for telescope azimuth, AZ_{enc} . Measurements will be made at $\simeq 1^\circ$ increments of azimuth. The two tiltmeters measuring tilt perpendicular to the elevation axle are averaged, and least-squares-fitted to a sinusoid to yield ζ_T and Φ_T (see below). These results should agree with the hydrostatic level system's calculations of the track tilt. The tilt component residuals left after removal of the sinusoid can then be used to produce a track model. Further measurement and analysis can be pursued if the amplitude of the tilt component residuals is significant. For example, there may exist higher harmonic terms as a function of azimuth such as the track terms in Table 1.

Finding the mean alidade track plane and track model by tiltmeters depends upon the fact that the alidade structure is almost rigid during azimuth rotations. The tiltmeter pairs at the two bearing ends are initially levelled when the telescope is at zero azimuth and rigging elevation angle (as recorded by the telescope axis encoders). If the alidade track is plane and the alidade structure rigid, the like-oriented tiltmeter pairs at the two ends of the alidade should read the same at every azimuth. A significant departure from equality would indicate alidade deformation, assuming that no significant temperature change of the structure occurred during the alidade rotation. Alidade structure bending would be implied for differences in the axially oriented tiltmeters; torsion would be implied by a difference in the tiltmeters oriented perpendicular to the elevation axle. Mean readings of the tiltmeters oriented in each direction would be used to obtain the mean alidade track plane angle parameters and the track model. The readings of the tiltmeter pairs oriented parallel to the elevation axis and those perpendicular to that axis should independently lead to the same track angle parameters.

Derivation of the track tilt parameters ζ_T and Φ_T in terms of tiltmeter data can be simplified by introducing the “alidade coordinate system”. The alidade structure is assumed to be a rigid structure with an embedded X_a, Y_a, Z_a coordinate system and mutually orthogonal unit frame vectors $\hat{X}_a, \hat{Y}_a, \hat{Z}_a$. Let Φ be the rotation angle of the alidade structure about telescope zenith from the position of zero azimuth encoder readout. If the azimuth encoder readout is linear then $\Phi = AZ_{enc}$. We will use Φ rather than AZ_{enc} as our azimuth angle variable, to allow for the possibility of later accounting separately for azimuth encoder non-linearity contributions to the pointing series.

The alidade coordinates can then be expressed in terms of the ground coordinate system (see Appendix B).

Tiltmeters are used to find track parameters ζ_T and Φ_T by the following procedure. The telescope is driven to commanded elevation $EL_{com} = EL_{rig} = 50.8^\circ$ (the telescope rigging angle) and commanded azimuth $AZ_{com} = 0^\circ$, which we refer to as the telescope reference position. The tiltmeters are supported on levelling screws which are set initially so that all tiltmeter readings become zero. That is, offset reference position reading angles of the tiltmeters are initialized to zero. The telescope is stepped in azimuth in 1° increments, and tilt readings are recorded. These readings give incremental tilt components of the elevation axis of the telescope with respect to its tilt position at the telescope reference position. As the telescope rotates in azimuth, the mean of the two axial tiltmeter readings for each tilt component varies to first approximation as a Fourier series.

The tiltmeter readout angles are given by τ_{ye} and τ_{xe} for tiltmeter orientation parallel to and perpendicular to the elevation axis, respectively. Calculations to analyze the tiltmeter measurements are given in Appendix C. They give the following result:

$$(3.2.01) \quad \tau_{xe}(\Phi) = -\zeta_T \cdot \cos \Phi_T + \zeta_T \cdot \cos \Phi_T \cdot (\cos \Phi) + \zeta_T \cdot \sin \Phi_T \cdot (\sin \Phi) \quad , \quad \text{and}$$

$$(3.2.02) \quad \tau_{ye}(\Phi) = -\zeta_T \cdot \sin \Phi_T + \zeta_T \cdot \sin \Phi_T \cdot (\cos \Phi) - \zeta_T \cdot \cos \Phi_T \cdot (\sin \Phi)$$

Tilt profiles $\tau_{xe}(\Phi)$ and $\tau_{ye}(\Phi)$ are least-squares-fitted by a three-term Fourier series to obtain track parameters ζ_T and Φ_T . The residuals produced from the difference between the model fit and the data provide a track model. Algorithms

for computation of Fourier coefficients are given in Appendix A.

We comment here on a particular feature of the measurements. The measurements, as just described, require that the tiltmeters always be levelled at standard azimuth as an initial condition. It is further implied, if not explicitly stated previously, that the alidade is thermally stable during the measurements, that is, it remains rigid. If those two conditions are fulfilled, the measurements will deliver the track parameters, independent of the actual alidade shape. If the alidade were to be heated non-uniformly before starting new measurements (so its shape departed from its earlier shape) tiltmeter readings at standard azimuth would depart from their previous level readings, and would thereby indicate a change in orientation of the elevation axle. New measurements, made with re-levelled tiltmeters, would deliver correct track parameters provided that the alidade were to maintain its new shape during the new measurements. (This however would be unlikely when alidade temperature was non-uniform or unstable).

0.3.3. Laser rangefinder measurements of targets on the box structure and feed arm

Ball retroreflector targets have been mounted under the box structure and on the horizontal and vertical feed arms. One or more ball retroreflectors have been positioned to lie on or close to the telescope's right-left plane of symmetry. When the tipping structure is moved in elevation, such a target should move accurately in a plane which can be determined by rangefinder measurements from the ground. Right-left deformations of the telescope (e.g. bending deformation of the elevation axle) should be near-symmetric and should not cause a midplane target's trajectory curve to depart significantly from planarity. (If trajectory measurements were to indicate a lack of planarity, they could be analyzed to provide additional pointing correction. Such a program will not be discussed in this document).

At a fixed azimuth the telescope will be stepped in elevation, typically in 1° increments. The unit normal vector to the target's plane of motion determines the direction of the elevation axis. The direction of the elevation axis, together with the alidade track tilt parameters, allows computation of the collimation pointing errors.

We may accurately determine the direction of the elevation axis with respect to the ground reference frame at an arbitrary alidade position (as indicated by AZ_{enc}), as follows (see Fig. 3). A ball target on the telescope tipping structure is tracked by ground rangefinders as tipping structure elevation is varied. After the range measurements have been reduced and least-squares adjusted by standard codes, the displacement vector between successive positions of the target's fiducial reference point (denoted by \widehat{D} in Fig. 3) is computed and normalized to unit magnitude. A sequence of unit target displacement vectors is generated as the target is tracked. Each of these unit displacement vectors lies in a plane perpendicular to the elevation axis of the telescope. The vector cross product of any two of these displacement vectors will be a unit vector in the direction of the elevation axis. By making multiple measurements on several targets one has a large set of measurement samples of the elevation axis unit vector, $\widehat{X}_r(AZ_{enc})$,

corresponding to the telescope azimuth during the measurements.

The geometry of the tipping structure of the GBT is described with reference to a “main reflector frame” having orthogonal unit basis vectors \hat{X}_r , \hat{Y}_r , \hat{Z}_r , and carrying a right-hand Cartesian coordinate system with coordinates X_r, Y_r, Z_r . This is a mathematical abstraction without specific reference to physical 3-space. To make the abstraction useful and unambiguous we must somehow embed the frame and coordinate system in physical space and have it carried along with the tipping structure as that structure moves in space and is driven in azimuth and elevation. To each azimuth and elevation of the telescope there must correspond unique direction cosines of the main-reflector-frame basis vectors with respect to the ground frame of the telescope.

This presents a conceptual problem which must be resolved. The tipping structure is not rigid. It deforms because of varying gravity moment torques as elevation is varied. When the elevation axle of the telescope is rotated in elevation by a specified angle, the axis of the “main reflector paraboloid” does not rotate by exactly the same angle. The main reflector may be a paraboloid at the start and finish of the elevation motion, but will not necessarily be the same paraboloid. The surface actuators may or may not be driven, which further complicates the conceptual problem. The elevation reference frame must somehow be embedded analytically into a deformable 3-dimensional continuum, that is a 3-dimensional differentiable manifold. This presents the problem. It can be uniquely stated and solved, however, provided that a finite element deformation model for the telescope is accepted. The orientation of a main reflector frame relative to the ground frame of reference of the telescope is obtained as the tipping structure moves in elevation and azimuth. The ground reference frame of the telescope, as determined by physical surveying methods, is considered to be invariant.

A method of doing this is given by [Wel 98] and [Gol 97]. One embeds a reference frame and coordinate system in physical space, to describe the deformable tipping structure’s geometry in the following way:

- The main reflector surface is physically set to conform to the design shape of the parent paraboloid when the elevation encoder output reads 50.8° , the “rigging elevation angle” of the telescope.
- The telescope is assumed to move as a rigid structure when it is driven

only in azimuth.

- By convention, the \widehat{X}_r frame vector and X_r -axis of coordinates point along the elevation axis of the telescope; unit frame vectors \widehat{Y}_r and \widehat{Z}_r are perpendicular to the elevation axis. The origin of the X_r, Y_r, Z_r main reflector coordinate system lies equidistant from the two elevation bearing centers. The elevation axis of the telescope is, then, a reference direction which defines the line of the main reflector coordinate system's X_r -axis. We note that if the alidade structure is rigid, and if one represents the unit vector \widehat{X}_r as a linear sum of alidade frame vectors: $\widehat{X}_r = c_1 \cdot \widehat{X}_a + c_2 \cdot \widehat{Y}_a + c_3 \cdot \widehat{Z}_a$, then the coefficients are independent of the alidade's azimuth angle.
- When the telescope is moved in azimuth only, motion of the embedded X_r, Y_r, Z_r frame and coordinate system in physical space is described in the following manner:

The main reflector frame is considered to be rigidly embedded in a rigid rotatable alidade structure resting, to first approximation, on a slightly tilted plane: the "Mean Alidade Track Plane (MATP)." The direction cosines describing the orientation of this plane are physically determined by means of fluid level measurements of track height or by tiltmeter measurements. The unit upward normal to this plane, \widehat{W} , is a fixed vector in physical 3-space, the "zenith vector of the GBT."

The X_a, Y_a, Z_a "alidade coordinate system" is rigidly embedded in the alidade structure. Its origin lies in the track plane (at the center of the annular alidade track). The Z_a -axis points along the fixed zenith vector \widehat{W} . (The physical track is actually bumpy. To deal with this, it is assumed to be plane but elevation corrections are added later using the track model obtained from track tilt residuals). Alidade rotations are described by the angle parameter Φ ($0 \leq \Phi < 2\pi$) the rotation in azimuth of the alidade structure. Unit vectors $\widehat{X}_a(\Phi), \widehat{Y}_a(\Phi)$ parallel to the mean track plane are defined so that $\widehat{X}_a(\Phi), \widehat{Y}_a(\Phi)$, and \widehat{W} form a right-hand orthogonal triple and also, $\widehat{X}_a(\Phi = 0) \cdot \widehat{Y} \equiv 0$.

Telescope azimuth is defined by the following requirement: When the alidade encoder output reading is zero, the \widehat{X}_a vector's projection onto the horizontal (local horizontal plane at the center of the azimuth track) has no component along \widehat{Y} .

The departure of the elevation axis orientation from that of an ideal telescope can be described in terms of two small-angle parameters (see Fig. 4). For a rigid alidade structure and a plane alidade track, when the alidade has been rotated to an azimuth angle Φ , about the telescope zenith axis, the direction of the elevation axis will be:

$$(3.3.01) \quad \widehat{X}_r(\Phi) = \widehat{X}_a(\Phi) \cdot \sqrt{1 - \beta_{el}^2 - \gamma_{el}^2} + \widehat{Y}_a(\Phi) \cdot (\gamma_{el}) - \widehat{Z}_a(\Phi) \cdot (\beta_{el}).$$

Here β_{el} and γ_{el} are small angular deviations of the elevation axis direction from the alidade frame vector directions. They are assumed to be constant during telescope motions. Angle β_{el} represents a deviation of the elevation axis from perpendicularity to the normal, \widehat{Z}_a , to the alidade track plane. The sign convention used is that the angle between the positive X_r -axis and the positive Z_a -axis is $\frac{\pi}{2} + \beta_{el}$. Angle γ_{el} is a deviation of the positive X_r -axis from the positive X_a -axis, towards the $+\widehat{Y}_a$ direction.

The direction vector of the elevation axis is expressed in terms of components relative to the ground reference frame, by substituting equations (B.01) and (B.10) into (3.3.01). This gives long, complicated expressions. For our purposes we need only first order approximation of these components. After extensive manipulation and reduction we get, to first order:

$$(3.3.02) \quad \begin{aligned} \widehat{X}_r(\Phi) = & \widehat{X} \cdot [(\cos \Phi) + (\gamma_{el}) \cdot (\sin \Phi)] \\ & + \widehat{Y} \cdot [(-\sin \Phi) + (\gamma_{el}) \cdot (\cos \Phi)] + \\ & + \widehat{Z} \cdot [(-\beta_{el}) + (\zeta_T) \cdot (\cos \Phi_T) \cdot (\sin \Phi) + (-\zeta) \cdot (\cos \Phi)]. \end{aligned}$$

This relation is a 4-parameter expression for $\widehat{X}_r(\Phi)$. Measurement data for $\widehat{X}_r(\Phi)$ is least-squares-fitted to give the four parameters. If track bumpiness is small,

$$(3.3.03) \quad \left(\frac{-1}{2}\right) \cdot (\widehat{Z}) \cdot (\widehat{X}_r(0^\circ) + \widehat{X}_r(180^\circ)) \simeq \beta_{el},$$

$$(3.3.04) \quad \left(\frac{1}{2}\right) \cdot (\widehat{Y}) \cdot (\widehat{X}_r(0^\circ) - \widehat{X}_r(180^\circ)) \simeq \gamma_{el},$$

The measured small angles β_{el} and γ_{el} correspond directly to the elevation axle collimation error and the azimuth zero, respectively (see [Wel 98] and the derivation in Appendix E). Explicitly,

$$(3.3.05) \quad b_{0,1}^{(AZ)} = -\beta_{EL}, \text{ and}$$

$$(3.3.06) \quad d_{0,1}^{(AZ)} = \gamma_{EL}.$$

0.4. Derivation of Pointing Corrections

After measuring telescope parameters: $\zeta_T, \Phi_T, \beta_{el}, \gamma_{el}$ we wish to compute the azimuth and elevation pointing series' which will be generated by non-zero values of these parameters and four additional parameters which we will define. Our goal is to generate "mechanical" pointing coefficients which can be used to give initial estimates for pointing series coefficients which are due to specific stable and long-term causes. The purpose of this program is to provide estimates of pointing coefficients before astronomical operation begins. It is expected that as the telescope begins its astronomical observations, and astronomical pointing coefficient determination starts, the a-priori coefficients will aid initial pointing and lead to small residues for the astronomically determined coefficients.

We next discuss how to generate the "mechanical" elevation and azimuth pointing series. We model two telescopes. Model-1 is an ideal design telescope. In Model-2 we introduce conceptual deviations from the ideal telescope.

We make the temporary assumption that telescope zenith coincides with the local upward gravity vertical direction. Ground coordinate frame vector directions $\hat{X}, \hat{Y}, \hat{Z}$ coincide, respectively, with astronomical East, astronomical North, and astronomical Zenith. (We later modify this to include deflection of local gravity vertical from geodetic zenith). Under this initial assumption, the spherical polar sky coordinates assigned to a direction in space are the same as the spherical polar ground coordinates with respect to the $\hat{X}, \hat{Y}, \hat{Z}$ ground reference frame.

Let us assume that the telescope is set to standard position, so the azimuth encoder reads $AZ_{enc} = 0$ and the elevation encoder reads rigging elevation angle EL_{rig} . We first assume that the GBT construction is perfect: alidade and tipping structures are rigid and invariant in shape and size, the main reflector surface is a region of a 60 meter focal length paraboloid, aligned so that the paraboloid's axis points to the \hat{X} direction and to elevation EL_{rig} with respect to the ground reference frame. When the telescope observing program requests that the telescope move to sky coordinates (AZ_{sky}, EL_{sky}) , the telescope commanded track, for this ideal telescope, will request motor drives to move to commanded telescope coordinates $EL_{com} = EL_{sky}$ and $AZ_{com} = AZ_{sky}$. After the alidade and tipping structure arrive at their requested positions, the azimuth encoder output reads $AZ_{enc} = AZ_{com}$ and the elevation encoder reads $EL_{enc} = EL_{com}$. The main

reflector is still a paraboloid of 60 meter focal length. Its axis points to the sky direction (AZ_{sky}, EL_{sky}) . This describes the behavior of our Model-1 ideal telescope.

For telescope Model-2 we introduce changes. Starting from the ideal telescope at standard position, we assume the following. The alidade is still rigid and has the ideal dimensions. The alidade track is still plane but is now tilted consistent with track parameters ζ_T and Φ_T . The elevation axle is twisted by the small angle β_{el} about the \hat{Y}_a direction and by the small angle γ_{el} about the \hat{Z}_a direction, leaving its midpoint fixed. The main reflector surface is still a region of a 60 meter focal length paraboloid when the telescope is at standard position (telescope azimuth encoder reads zero and the telescope elevation encoder reads EL_{rig}).

For the Model-1 ideal design telescope we have assumed that the main reflector paraboloid has been initially adjusted so when it is at standard position, its axis points in the direction: $\hat{Q}_0 \iff (AZ_{sky} = 0, EL_{sky} = EL_{rig})$.

For the Model-2 telescope we now assume that the main reflector paraboloid has been initially adjusted as built so when at standard position, its axis points in the direction: $\hat{P}_0 \iff (AZ_{sky} = A_0, EL_{sky} = EL_{rig} + E_0)$. Here A_0 and E_0 are small angles, typically less than 10 arc-minutes. We temporarily neglect the deviation of local gravity vertical from geodetic zenith. In principle, A_0 and E_0 could be directly measured by laser rangefinder determinations of the paraboloid shape and orientation with respect to the ground reference frame of the telescope.

For the Model-2 telescope we make the following assumptions about the shape and orientation of the main reflector surface when the tipping structure is driven to change its elevation: The telescope elevation axis remains straight and unbent. The main reflector surface is always a patch on a paraboloid of revolution. As tipping structure elevation changes the reflector surface remains paraboloidal but is no longer rigid. Focal length becomes a function of elevation (as read out by the elevation encoder). The angle that the axis of the instantaneous paraboloid makes with the elevation axis is fixed; that is, the paraboloid axis can be considered rigid and welded solidly to the rigid elevation axis. We also make a peculiar assumption: when the tipping structure is driven from encoder elevation $EL_{enc} = EL_{rig}$ to encoder elevation $EL_{enc} = EL_{com}$, the main surface paraboloid's axis direction rotates about the elevation axis not by incremental angle $(EL_{com} - EL_{rig})$, but instead by the incremental angle $(EL_{com} - EL_{rig} + E_{grav})$, where E_{grav} is assumed

to be a known function of EL_{enc} .

We introduce function $EL_{grav}(EL_{enc})$ to serve the following purpose. The telescope's tipping structure is not rigid. The main reflector surface must be re-adjusted to remain paraboloidal as tipping structure elevation changes, according to a schedule which is theoretically calculated (using the current Finite Element Model of the tipping structure). As elevation changes, the axis of this instantaneous paraboloid does not follow the rotation as indicated by the elevation encoder, but lags or leads by an angle increment which can be calculated as a function of encoder readout angle. The calculational program has been carried out by D. Wells [Wel 98].

The gravity elevation function, in the notation of Wells, is written:

$$(4.01) \quad r_x(EL) = d_{0,0}^{EL} + d_{0,1}^{EL} \cdot \cos EL + b_{0,1}^{EL} \cdot \sin EL.$$

Explicit values for this function are given in [Wel 98]. It takes value zero at $EL = EL_{rig}$. At present it is not appropriate to use the $d_{i,j}^{EL}$ notation for the above coefficient names, because we have not yet demonstrated that they are, in fact, Condon model pointing coefficients.

We prefer to write (4.01) as:

$$(4.02) \quad EL_{grav}(EL_{enc}) = \rho_0 + \rho_c \cdot \cos EL_{enc} + \rho_s \cdot \sin EL_{enc}, \text{ where}$$

$$(4.03) \quad \rho_0 + \rho_c \cdot \cos EL_{rig} + \rho_s \cdot \sin EL_{rig} \equiv 0, \quad \text{which gives}$$

$$(4.04) \quad EL_{grav}(EL_{enc}) = \rho_c \cdot (\cos EL_{enc} - \cos EL_{rig}) + \rho_s \cdot (\sin EL_{enc} - \sin EL_{rig}).$$

We will later use first order approximations

$$(4.05) \quad \sin EL_{grav}(EL_{enc}) = EL_{grav}(EL_{enc}), \quad \cos EL_{grav}(EL_{enc}) = 1.$$

We have defined two telescopes, and specified their initial pointing at standard position. Pointing at arbitrary commanded azimuth and elevation depends upon four measured parameters $\zeta_T, \Phi_T, \beta_{el}, \gamma_{el}$ discussed previously, together with additional parameters $EL_{rig}, A_0, E_0, \rho_c, \rho_s$. We next compute the pointing

when the telescopes are commanded to move to arbitrary encoder coordinates (AZ_{com}, EL_{com}) .

To do this we first rotate the initial paraboloid axis vector, \hat{P}_0 , about the tilted elevation axis (see Fig. 5)

$$(4.06) \quad \hat{X}_r(\Phi = 0) = \hat{X} + \hat{Y} \cdot [\gamma_{el}] + \hat{Z} \cdot [-\beta_{el} + (-\zeta_T) \cdot (\sin \Phi_T)],$$

by the angle:

$$(4.07) \quad Rot_1 = EL_{com} - EL_{rig} + EL_{grav}(EL_{com}).$$

This carries the paraboloid's axis direction from \hat{P}_0 to a new direction, \hat{P}_1 .

We then rotate vector \hat{P}_1 about the telescope zenith \hat{W} , by the angle $Rot_2 = \Phi$. ($\Phi = AZ_{com}$ when the azimuth encoder is linear). The paraboloid axis then arrives at the direction \hat{P} . The deviations in azimuth and elevation of the direction of \hat{P} from the commanded azimuth and elevation gives the required pointing corrections. The corrections appear as harmonic series in commanded azimuth and elevation. The coefficients in these series are functions of the eight parameters mentioned above. Term coefficients are of first order in small angle parameters. By identifying harmonic coefficients of the "mechanical" pointing series (obtained by carrying out the algebra for the above rotations) one-to-one with Condon's series coefficients, we obtain a set of *a-priori* estimators for the pointing coefficients. Finally, we will compute additional contributions caused by track bumpiness (using track model residues) and by departure of local gravity vertical from astronomical zenith.

We carry out the algebraic computation of direction \hat{P} and express the result in spherical polar coordinates in the ground reference frame, in Appendix E. The rotation geometry is shown in Fig. 5. When ground frame Cartesian components of \hat{P} are available, computation of the pointing series is straightforward, and proceeds as follows.

One compares the computed components of \hat{P} with those expected for successive rotations of an ideal telescope, $(EL_{com} - EL_{rig})$ in elevation and AZ_{com} in azimuth, of unit direction vector \hat{Q}_0 . Vector \hat{Q}_0 has polar coordinates $(0, EL_{rig})$

with respect to the ground frame. It is carried by the two rotations to a unit vector whose polar coordinates are (AZ_{com}, EL_{com}) with respect to the ground frame. The Cartesian ground frame coordinates of the two-fold rotated vector, \hat{Q} , are $(\sin AZ_{com} \cdot \cos EL_{com}, \cos AZ_{com} \cdot \cos EL_{com}, \sin EL_{com})$. These would be the Cartesian coordinates of \hat{P} if the telescope were ideal. As-built telescope imperfections, described by non-zero first order parameters, cause \hat{P}_0 to arrive, after successive rotations about canted axes, at a direction whose ground frame coordinates are:

$$(4.08) \quad P_X = \sin AZ \cdot \cos EL, \quad P_Y = \cos AZ \cdot \cos EL, \quad P_Z = \sin EL,$$

where AZ and EL are spherical polar coordinates of \hat{P} relative to the ground reference frame. If the Cartesian ground coordinates of unit vector \hat{P} are changed by small increments dP_X, dP_Y, dP_Z , then its ground-frame-related polar coordinates change by increments dAZ, dEL . Differentiating (4.08), the small increments in the Cartesian coordinates of \hat{P} are related to changes in its polar coordinates by

$$(4.09) \quad dP_X = (\cos AZ) \cdot (\cos EL) \cdot dAZ - (\sin AZ) \cdot (\sin EL) \cdot dEL,$$

$$(4.10) \quad dP_Y = -(\sin AZ) \cdot (\cos EL) \cdot dAZ - (\cos AZ) \cdot (\sin EL) \cdot dEL,$$

$$(4.11) \quad dP_Z = (\cos EL) \cdot dEL,$$

$$(4.12) \quad P_X \cdot dP_X + P_Y \cdot dP_Y + P_Z \cdot dP_Z = 0, \quad \text{which give}$$

$$(4.13) \quad dEL = (\sec EL) \cdot dP_Z,$$

$$(4.14) \quad (\cos EL) \cdot dAZ = (\sec AZ) \cdot dP_X + (\tan AZ) \cdot (\tan EL) \cdot dP_Z.$$

If the as-built telescope were perfect and all first order parameters vanished, the coordinates of \hat{P} would be:

$$(4.15) \quad P_X = \sin AZ_{com} \cdot \cos EL_{com} = Q_X,$$

$$P_Y = \cos AZ_{com} \cdot \cos EL_{com} = Q_Y, \quad P_Z = \sin EL_{com} = Q_Z.$$

The deviations dP_X, dP_Y, dP_Z , of the components of \hat{P} (for the as-built telescope) from those of \hat{Q} are computed in terms of the telescope parameters, in Appendix E. The shifts in elevation and azimuth of \hat{P} from those of the perfect telescope are then given by:

$$(4.16) \quad dEL = (\sec EL_{com}) \cdot dP_Z ,$$

$$(4.17) \quad (\cos EL_{com}) \cdot dAZ = (\sec AZ_{com}) \cdot dP_X + \\ + (\tan AZ_{com}) \cdot (\tan EL_{com}) \cdot dP_Z .$$

The right hand sides of equations (4.16) and (4.17) turn out to be linear sums in products of sines and cosines of the harmonics of AZ_{com} with those of EL_{com} . These give our mechanical pointing series in elevation and azimuth. The negatives of those shifts are the pointing corrections. That is:

$$(4.18) \quad \Delta EL = -(\sec EL_{com}) \cdot dP_Z ,$$

$$(4.19) \quad (\cos EL_{com}) \cdot \Delta AZ = -(\sec AZ_{com}) \cdot dP_X + \\ - (\tan AZ_{com}) \cdot (\tan EL_{com}) \cdot dP_Z .$$

The explicit computations are given in Appendix E. The results are given in Table 1b. The results do not include the correction for the deviation of local gravity vertical from the local normal to the geodetic azimuth. That correction is given separately in Appendix F.

Table 1b. Estimated Pointing Coefficients.

(Not including geodetic corrections)

$\Delta A \cos E$ (Azimuth Pointing Series Terms)			
Coeff	Term	Meaning	Estimated Value (radian)
$d_{0,0}^{(AZ)}$	1	Hor. Col.	$-A_0 \cdot \cos EL_{rig} - \gamma_{el} \cdot \cos EL_{rig}$ $+\beta_{el} \cdot \sin EL_{rig} + \zeta_T \cdot \sin \Phi_T \cdot \sin EL_{rig}$
$b_{0,1}^{(AZ)}$	$\sin E$	El. Ax. Col.	$-\beta_{el}$
$d_{0,1}^{(AZ)}$	$\cos E$	Az Zero	γ_{el}
$d_{1,1}^{(AZ)}$	$\cos A \cos E$	Az Enc	See Appendix D
$c_{1,1}^{(AZ)}$	$\sin A \cos E$	Az Enc	See Appendix D
$b_{1,1}^{(AZ)}$	$\cos A \sin E$	Zen E -Tilt	$-\zeta_T \cdot \sin \Phi_T$
$a_{1,1}^{(AZ)}$	$\sin A \sin E$	Zen N -Tilt	$\zeta_T \cdot \cos \Phi_T$
$c_{2,1}^{(AZ)}$	$\sin 2A \cos E$	Az Track	See Appendix D
$d_{2,1}^{(AZ)}$	$\cos 2A \cos E$	Az Track	See Appendix D

ΔE (Elevation Pointing Series Terms)			
Coeff	Term	Meaning	Estimated Value (radian)
$d_{0,0}^{(EL)}$	1	Elev Zero	$-E_0 - \zeta_T \cdot \cos \Phi_T$ $+\rho_c \cdot \cos EL_{rig} + \rho_s \cdot \sin EL_{rig}$
$c_{1,0}^{(EL)}$	$\sin A$	Zen E -Tilt	$\zeta_T \cdot \sin \Phi_T$
$d_{1,0}^{(EL)}$	$\cos A$	Zen N -Tilt	$\zeta_T \cdot \cos \Phi_T$
$b_{0,1}^{(EL)}$	$\sin E$	Asym Gravity	$-\rho_s$
$d_{0,1}^{(EL)}$	$\cos E$	Symm Gravity	$-\rho_c$

0.5. Least-squares Analysis Of Metrology Data

The algorithm for finding the track zenith and azimuth is given in Appendix A. It is basically the same as has been used for reducing laser rangefinder data, and provides good accuracy. The algorithm is easily extended to examine the track fluid level and tiltmeter data for significant higher harmonic terms. A similar algorithm for second harmonic terms can be applied to the orientation data for the sub-bearing target balls to look for the presence of significant azimuth track $\sin 2A \cdot \cos E$ and $\cos 2A \cdot \cos E$ coefficients and azimuth track terms of higher harmonic content.

The reduction of ball trajectory position data to find the best fitted plane for the measured trajectory points is a standard statistical problem. The desired plane is that which minimizes the sum of the normal distances squared of the measurement sample points to a general plane. The unit normal vector to this least-squares-fit plane is the elevation axis. The normal distance residuals of the sample points from this plane can be examined as a function of elevation, to see if there is a statistically significant trend indicating that the axis may be changing with elevation.

0.6. Summary Of Pointing Coefficients

The pointing coefficients are listed below, with a summary of their determination by metrologic means:

$d_{0,0}^{(AZ)}$	1	Horizontal Collimation	$-A_0 \cdot \cos EL_{rig} - \gamma_{el} \cdot \cos EL_{rig}$ $+ \beta_{el} \cdot \sin EL_{rig} + \zeta_T \cdot \sin \Phi_T \cdot \sin EL_{rig}$
------------------	---	------------------------	--

This coefficient contains offsets due to track tilt, elevation axis horizontal offset, and paraboloid surface initial horizontal offset. Determination of all parameters except A_0 is discussed in the text or appendices. The main reflector offset A_0 can, in principle, be measured as follows. The antenna is brought to standard position. Feed arm laser rangefinders are located by ranging from the ground. Main reflector surface points locations are then determined by trilateration from the feed arm rangefinders. To accomplish this, surface retroreflector target locations are corrected to give surface point locations. The surface is then least-squares-fitted to a 10-parameter quadric, a paraboloid. The axis of this paraboloid is then computed, and referenced to the ground coordinate frame to give parameters A_0 and E_0 . Practically, this coefficient is easily found by astronomical pointing. Its determination by measurement of the main reflector surface is not usually needed, and is of some complexity.

$b_{0,1}^{(AZ)}$	$\sin E$	Elevation Axis. Collimation	$-\beta_{el}$
------------------	----------	-----------------------------	---------------

The elevation axis collimation term is due to tilt of the elevation axis from the horizontal caused by non-perpendicularity of the elevation and azimuth axes of the telescope. The coefficient is measured by determining the normal vector to the mean plane generated by a midplane ball retroreflector, ranged from the ground.

$d_{0,1}^{(AZ)}$	$\cos E$	Azimuth Zero	$\gamma_{el} + \eta \cdot \tan \phi$
------------------	----------	--------------	--------------------------------------

The parameter γ is found by determining the normal vector to the plane gen-

erated by an orthogonal distance regression fit to the locations measured for a midplane ball retroreflector ranged from the ground, as telescope elevation is varied. An additional contribution to the commanded pointing appears: the horizontal Laplace correction, required to shift commanded pointing from astronomical reference to geodetic reference. The value of parameter η is given in Appendix F. Parameter ϕ is the geodetic latitude of the alidade track top center of the GBT, and is also given in Appendix F.

$$\boxed{b_{1,1}^{(AZ)} \quad \cos A \sin E \quad \text{Zenith E-Tilt} \quad -\zeta_{TX} - \eta = -\zeta_T \cdot \sin \Phi_T - \eta}$$

This coefficient is due to two independent contributors: track tilt and astronomical-to-geodetic frame correction. The latter correction behaves as an additional track tilt, together with a constant azimuth shift (the horizontal Laplace term). The term η is a constant (for the GBT) which is the “prime vertical” component of the gravity deflection of astronomical zenith relative to geodetic zenith at GBT. Its value is given in Appendix F. The track component of the coefficient is obtained by least squares fit of fluid level measurements of track elevation to a 3-term Fourier series. It is also obtained independently by a similar fit of tiltmeter measurements. The value in radians is used.

$$\boxed{a_{1,1}^{(AZ)} \quad \sin A \sin E \quad \text{Zenith N-Tilt} \quad \zeta_{TY} + \xi = \zeta_T \cdot \cos \Phi_T + \xi}$$

This coefficient is due to two independent contributors: track tilt and astronomical-to-geodetic frame correction. The latter correction behaves as an additional track tilt together with a constant azimuth shift. The parameter ξ is a constant (for the GBT), the meridian component of the gravity deflection relative to geodetic zenith at GBT. Its value is given in Appendix F. The value in radians is used in the coefficient. The track tilt contribution for this pointing coefficient is obtained by least squares fit of fluid level measurements of track elevation to a 3-term Fourier series. It is also obtained independently by a similar fit of tiltmeter measurements.

$$\boxed{c_{2,1}^{(AZ)} \quad \sin 2A \cos E \quad \text{Azimuth Track}}$$

$$\boxed{d_{2,1}^{(AZ)} \quad \cos 2A \cos E \quad \text{Azimuth Track}}$$

These coefficients are due to track deviation from planarity. They can be obtained from a least squares fit of second harmonic terms of the track rotation

angle versus azimuth encoder readout derived from measurements of a reference line direction defined by four alidade target balls under the bearing platforms. The nature of the series term is discussed in [Con 92] and Appendix D. The detailed values will be derived in a later note.

$$\boxed{d_{0,0}^{(EL)} \quad 1 \quad \text{Elevation Zero} \quad \begin{aligned} & -E_0 + \rho_c \cdot \cos EL_{rig} \\ & + \rho_s \cdot \sin EL_{rig} - \zeta_T \cdot \cos \Phi_T \end{aligned}}$$

This coefficient contains offsets due to track tilt, gravity elevation offset to initialize the gravity deformation to be set to zero at the rigging elevation, paraboloid surface initial elevation offset. Its determination is by the same procedure as for $d_{0,0}^{(AZ)}$. Practically, it is easily found by astronomical pointing. Its determination by measurement of the main reflector surface is not usually needed, and is of some complexity.

$$\boxed{c_{1,0}^{(EL)} \quad \sin A \quad \text{Zenith E-Tilt} \quad \zeta_{TX} + \eta = \zeta_T \cdot \sin \Phi_T + \eta}$$

The value of ζ_{TX} is obtained by a three term least squares Fourier series fit to track fluid level elevation data or tiltmeter data. The value of η is given in Appendix F.

$$\boxed{d_{1,0}^{(EL)} \quad \cos A \quad \text{Zenith N-Tilt} \quad \zeta_{TY} + \xi = \zeta_T \cdot \cos \Phi_T + \xi}$$

The value of ζ_{TY} is obtained by a three term least squares Fourier series fit to track fluid level elevation data or tiltmeter data. The value of ξ is given in Appendix F.

$$\boxed{b_{0,1}^{(EL)} \quad \sin E \quad \text{Asymmetric Gravity} \quad -\rho_s}$$

This coefficient was computed by D. Wells [Wel 95], based on the Finite Element Model of the GBT tipping structure. (It requires recomputation, however, to correct for the change of elevation rigging angle to 50.8° , from the value of 44° assumed in 1995). It depends on appropriate reshaping of the main reflector surface with elevation and is not directly measurable. It is however possible to verify or correct the F.E.M. gravity deflections which determine the coefficient. This can be done by an analysis of the midplane ball trajectory position data measured by ground rangefinders when the tipping structure elevation is varied.

$d_{1,1}^{(EL)}$	$\cos E$	Symmetric Gravity	$-\rho_c$
------------------	----------	-------------------	-----------

See remarks above relating to $b_{0,1}^{(EL)}$.

Appendix A. Hydrostatic Level Analysis Of The Azimuth Track

An algorithm useful to fit a sine wave to a set of n elevation samples $h_j(\phi_j)$, ($\phi_j = \frac{2\pi \cdot j}{n}$, $j = 0, \dots, n-1$), uniformly spaced about the track is:

$$(A.01) \quad \langle h \rangle_{av} = \left(\frac{1}{n} \right) \cdot \sum_{j=0}^{n-1} (h_j) \quad ,$$

$$(A.02) \quad A = \left(\frac{1}{n} \right) \cdot \sum_{j=0}^{n-1} (h_j - \langle h \rangle_{av}) \cdot \cos(\phi_j) \quad ,$$

$$(A.03) \quad B = \left(\frac{1}{n} \right) \cdot \sum_{j=0}^{n-1} (h_j - \langle h \rangle_{av}) \cdot \sin(\phi_j) \quad ,$$

$$(A.04) \quad H_1 = \left(\frac{2}{n} \right) \cdot \sqrt{A^2 + B^2} \quad ,$$

$$(A.05) \quad \Phi_{min} = -\tan^{-1} \left(\frac{B}{A} \right) \quad .$$

Here, Φ_{min} is the fitted azimuth of minimum track elevation found for the data samples. For the track data fit, $\Phi_{min} = \Phi_T$.

To fit higher harmonics to sampled data one can use:

$$(A.06) \quad A_m = \left(\frac{1}{n} \right) \cdot \sum_{j=0}^{n-1} (h_j - \langle h \rangle_{av}) \cdot \cos(m \cdot \phi_j) \quad ,$$

$$(A.07) \quad B_m = \left(\frac{1}{n} \right) \cdot \sum_{j=0}^{n-1} (h_j - \langle h \rangle_{av}) \cdot \sin(m \cdot \phi_j) \quad .$$

Appendix B. Alidade Coordinate System.

The telescope zenith vector is a fixed vector having spherical coordinates (ζ_T, Φ_T) relative to the ground reference frame of the telescope. In the Cartesian ground frame coordinate system it has representation:

$$(B.01) \quad \widehat{W} = \widehat{X} \cdot [\sin \zeta_T \cdot \sin \Phi_T] + \widehat{Y} \cdot [\sin \zeta_T \cdot \cos \Phi_T] + \widehat{Z} \cdot [\cos \zeta_T] .$$

The alidade reference frame vector \widehat{Z}_a is fixed, and

$$(B.02) \quad \widehat{Z}_a(\Phi = 0) \equiv \widehat{W} .$$

When the telescope azimuth is zero (as read out by the azimuth encoder) we choose arbitrarily: $\Phi \equiv 0$ and $AZ_{enc} \equiv 0$. At zero azimuth, the frame vector $\widehat{X}_a(\Phi = 0)$ is determined by the conditions that it is \perp to \widehat{W} and has no component towards North. That is, we choose arbitrarily:

$$(B.03) \quad \widehat{X}_a(\Phi = 0) \cdot \widehat{W} = 0 , \quad \text{and} \quad \widehat{X}_a(\Phi = 0) \cdot \widehat{Y} = 0 .$$

The second of these implies that we can write

$$(B.04) \quad \widehat{X}_a(\Phi = 0) = \sqrt{1 - \zeta^2} \cdot \widehat{X} - \zeta \cdot \widehat{Z}$$

where ζ is small and to be determined. The first condition then implies

$$(B.05) \quad \sqrt{1 - \zeta^2} \cdot (\sin \zeta_T \cdot \sin \Phi_T) - \zeta \cdot (\cos \zeta_T) = 0 , \quad \text{which gives}$$

$$(B.06) \quad \frac{\zeta}{\sqrt{1 - \zeta^2}} = \tan \zeta_T \cdot \sin \Phi_T .$$

Because track tilt ζ_T is small, we can use first order approximation, and with negligible loss of accuracy set:

$$(B.07) \quad \zeta = \zeta_T \cdot \sin \Phi_T .$$

Frame vector $\widehat{Y}_a(\Phi = 0)$ is determined by the orthogonality relation

$$(B.08) \quad \widehat{Y}_a(\Phi = 0) \equiv \widehat{Z}_a(\Phi = 0) \times \widehat{X}_a(\Phi = 0).$$

Expanding the vector product gives

$$(B.09) \quad \begin{aligned} \widehat{Y}_a(\Phi = 0) &= \widehat{X} \cdot [(-\zeta) \cdot (\sin \zeta_T) \cdot (\cos \Phi_T)] \\ &+ \widehat{Y} \cdot [(\zeta) \cdot (\sin \zeta_T) \cdot (\sin \Phi_T) + (\cos \Phi_T) \cdot \sqrt{1 - \zeta^2}] + \\ &+ \widehat{Z} \cdot [(-\sin \zeta_T) \cdot (\cos \Phi_T) \cdot \sqrt{1 - \zeta^2}]. \end{aligned}$$

At arbitrary azimuth, Φ , the unit frame vectors are:

$$(B.10a) \quad \widehat{X}_a(\Phi) = \widehat{X}_a(\Phi = 0) \cdot \cos \Phi - \widehat{Y}_a(\Phi = 0) \cdot \sin \Phi,$$

$$(B.10b) \quad \widehat{Y}_a(\Phi) = \widehat{X}_a(\Phi = 0) \cdot \sin \Phi + \widehat{Y}_a(\Phi = 0) \cdot \cos \Phi,$$

$$(B.10c) \quad \widehat{Z}_a(\Phi) = \widehat{W}.$$

Substituting (B.08) and (B.09) into equations (B.10) gives:

$$(B.11a) \quad \begin{aligned} \widehat{X}_a(\Phi) &= \widehat{X} \cdot [\sqrt{1 - \zeta^2} \cdot (\cos \Phi) + (\zeta) \cdot (\sin \zeta_T) \cdot (\cos \Phi_T) \cdot (\sin \Phi)] \\ &+ \widehat{Y} \cdot [(-\zeta) \cdot (\sin \zeta_T) \cdot (\cos \Phi_T) \cdot (\sin \Phi) - \sqrt{1 - \zeta^2} \cdot (\cos \zeta_T) \cdot (\sin \Phi)] + \\ &+ \widehat{Z} \cdot [(\sin \zeta_T) \cdot \sqrt{1 - \zeta^2} \cdot (\cos \Phi_T) \cdot (\sin \Phi) - (\zeta) \cdot (\cos \Phi)]. \end{aligned}$$

$$(B.11b) \quad \begin{aligned} \widehat{Y}_a(\Phi) &= \widehat{X} \cdot [\sqrt{1 - \zeta^2} \cdot (\sin \Phi) + (-\zeta) \cdot (\sin \zeta_T) \cdot (\cos \Phi_T) \cdot (\cos \Phi)] \\ &+ \widehat{Y} \cdot [(\zeta) \cdot (\sin \zeta_T) \cdot (\cos \Phi_T) \cdot (\cos \Phi) + \sqrt{1 - \zeta^2} \cdot (\cos \zeta_T) \cdot (\cos \Phi)] + \\ &+ \widehat{Z} \cdot [(-\sin \zeta_T) \cdot \sqrt{1 - \zeta^2} \cdot (\cos \Phi_T) \cdot (\cos \Phi) + (-\zeta) \cdot (\sin \Phi)]. \end{aligned}$$

To first order:

$$(B.12a) \quad \widehat{X}_a(\Phi) = \widehat{X} \cdot [\cos \Phi] + \widehat{Y} \cdot [-\sin \Phi] + \\ + \widehat{Z} \cdot [(\zeta_T) \cdot (\cos \Phi_T) \cdot (\sin \Phi) + (-\zeta_T) \cdot (\sin \Phi_T) \cdot (\cos \Phi)].$$

$$(B.12b) \quad \widehat{Y}_a(\Phi) = \widehat{X} \cdot [\sin \Phi] + \widehat{Y} \cdot [\cos \Phi] + \\ + \widehat{Z} \cdot [(-\zeta_T) \cdot (\cos \Phi_T) \cdot (\cos \Phi) + (-\zeta_T) \cdot (\sin \Phi_T)(\sin \Phi)].$$

$$(B.12c) \quad \widehat{Z}_a(\Phi) = \widehat{X} \cdot [(\zeta_T) \cdot (\sin \Phi_T)] + \widehat{Y} \cdot [(\zeta_T) \cdot (\cos \Phi_T)] + \widehat{Z} \cdot [1].$$

Appendix C. Track Model And Tilt Parameter Determination

Four tiltmeters will be placed on the alidade bearing platforms, two near each elevation axle. For small tilts, each behaves as an ideal 1-axis tiltmeter, which is a frictionless mechanism of the following nature. A base plane (considered to be a rigid plate) has two perpendicular lines on it. One of these is defined to be the axis of a pendulum. The other is defined to be the direction axis of the instrument. At their intersection a joint is attached which allows a pendulum weight bob, suspended on a line of fixed length, to oscillate freely in a plane perpendicular to both the base plane and the pendulum axis. It does not however allow motion perpendicular to that plane. The deviation angle of the bob's support line from the normal to the base plane is the observed tilt angle (with a suitable chosen sign convention). When the base plane is near horizontal, the observed tilt angle gives an accurate estimate of the inclination angle of the instrument's direction axis to horizontal. The tilt angle is, however, insensitive to the inclination of the pendulum axis to the horizontal.

Tiltmeter orientations are shown in Fig. 2. Instrument T_1 is oriented to be sensitive to elevation rotations of the alidade, and is located with $X_r(T_1) > 0$. Tiltmeter T_3 will also be oriented to be sensitive to elevation rotations of the alidade, but is placed at the opposite bearing, $X_r(T_3) < 0$. Tiltmeter T_2 is oriented to be sensitive to rotations about a horizontal line perpendicular to the elevation axis, and is located at the same bearing as T_1 , $X_r(T_2) > 0$. Tiltmeter T_4 has the same orientation as T_2 and is located at the same bearing as T_3 , so $X_r(T_4) < 0$.

All tiltmeters are simultaneously levelled when the telescope is brought to the standard position defined by: $EL_{enc} = EL_{rig}$, $AZ_{enc} = 0$, $\Phi = 0$. Tiltmeter pairs will be placed on suitable base plates and calibrated in the Green Bank optical calibration laboratory so that their orientations and orthogonality and zero tilt calibration are well-determined in the laboratory. The tiltmeters may subsequently be installed on the GBT with accurate alignment along and perpendicular to the elevation axis. Each 2-axis tiltmeter will be placed in an instrument package (possibly temperature regulated) which can be pinned and bolted to a bracket on the alidade structure near the elevation axis, together with instrumentation and power cables.

Each instrument package will be provided with a temporary mount for a small alignment telescope, to set directions of T_1 and T_3 parallel to the elevation axle.

Before starting measurements, the GBT will be brought to standard position and all four tiltmeters will be levelled. The instrument behavior is described as follows. A unit vector, $\hat{T}_i(\Phi)$, is associated to each tiltmeter ($i = 1, 2, 3, 4$). The observed instrument readout gives its tilt angle, either $\tau_{xe}(\Phi)$ about the $X_e(\Phi)$ -axis, or $\tau_{ye}(\Phi)$ about the $Y_e(\Phi)$ -axis. The expected instrument readouts are given in Table 2.

Table 2.

Meter	Readout Angle	Standard Position Direction Of Instrument Axis $\hat{T}_i(\Phi = 0)$	Direction Of Instrument Axis $\hat{T}_i(\Phi) =$ $t_{ix}\hat{X} + t_{iy}\hat{Y} + t_{iz}\hat{Z}$	Instrument Axis Angle To Horizontal (Readout Angle)
T_1	$\tau_{xe}(\Phi)$	$-\hat{Y}$	$\hat{T}_1(\Phi)$	$\frac{t_{1z}(\Phi)}{\sqrt{(t_{1x}(\Phi))^2 + (t_{1y}(\Phi))^2}}$
T_2	$\tau_{ye}(\Phi)$	$-\hat{X}$	$\hat{T}_2(\Phi)$	$\frac{t_{2z}(\Phi)}{\sqrt{(t_{2x}(\Phi))^2 + (t_{2y}(\Phi))^2}}$
T_3	$\tau'_{xe}(\Phi)$	$-\hat{Y}$	$\hat{T}_3(\Phi)$	$\frac{t_{3z}(\Phi)}{\sqrt{(t_{3x}(\Phi))^2 + (t_{3y}(\Phi))^2}}$
T_4	$\tau'_{ye}(\Phi)$	$-\hat{X}$	$\hat{T}_4(\Phi)$	$\frac{t_{4z}(\Phi)}{\sqrt{(t_{4x}(\Phi))^2 + (t_{4y}(\Phi))^2}}$

Assume a plane track. For $\Phi = 0$, the instrument axis direction vectors are initially,

$$(C.01) \quad \hat{T}_i(0) = \{ \hat{X}_a(0) \cdot [\hat{T}_i(0) \cdot \hat{X}_a(0)] + \hat{Y}_a(0) \cdot [\hat{T}_i(0) \cdot \hat{Y}_a(0)] + \hat{Z}_a(0) \cdot [\hat{T}_i(0) \cdot \hat{Z}_a(0)] \}.$$

This gives:

$$(C.02) \quad \hat{T}_1(0) = \hat{T}_3(0) = -\hat{Y} = \hat{Y}_a(0) \cdot [(-\zeta) \cdot (\sin \zeta_T) \cdot (\sin \Phi_T) + (-\cos \zeta_T) \cdot \sqrt{1 - \zeta^2}] + \hat{Z}_a(0) \cdot [(-\sin \zeta_T) \cdot (\cos \Phi_T)] .$$

$$(C.03) \quad \hat{T}_2(0) = \hat{T}_4(0) = -\hat{X} = \{ \hat{X}_a(0) \cdot (-\sqrt{1 - \zeta^2}) \} + \{ \hat{Y}_a(0) \cdot [(\zeta) \cdot (\sin \zeta_T) \cdot (\cos \Phi_T)] + \hat{Z}_a(0) \cdot [(-\sin \zeta_T) \cdot (\sin \Phi_T)] \} .$$

After the alidade rotates about telescope zenith by angle Φ the instrument axis direction vectors become, for the case of a plane track:

$$(C.04) \quad \hat{T}_1(\Phi) = \hat{T}_3(\Phi) = \hat{Y}_a(\Phi) \cdot [(-\zeta) \cdot (\sin \zeta_T) \cdot (\sin \Phi_T) + (-\cos \zeta_T) \cdot \sqrt{1 - \zeta^2}] + \hat{Z}_a(\Phi) \cdot [(-\sin \zeta_T) \cdot (\cos \Phi_T)] .$$

$$(C.05) \quad \hat{T}_2(\Phi) = \hat{T}_4(\Phi) = \hat{X}_a(\Phi) \cdot (-\sqrt{1 - \zeta^2}) + \hat{Y}_a(\Phi) \cdot [(\zeta) \cdot (\sin \zeta_T) \cdot (\cos \Phi_T)] + \hat{Z}_a(\Phi) \cdot [(-\sin \zeta_T) \cdot (\sin \Phi_T)] .$$

These direction vectors are expressed in terms of ground frame basis vectors \hat{X} , \hat{Y} , \hat{Z} by substituting expressions (B.12) for the alidade frame basis vectors. After some manipulation, the direction vectors, to first order in small angles reduce to

$$(C.06) \quad \hat{T}_1(\Phi) = \hat{T}_3(\Phi) = \hat{X} \cdot [-\sin \Phi] + \hat{Y} \cdot [-\cos \Phi] + \\ + \hat{Z} \cdot [(\zeta_T) \cdot (\cos \Phi_T) \cdot (-1 + \cos \Phi) + (\zeta_T) \cdot (\sin \Phi_T) \cdot (\sin \Phi)].$$

$$(C.07) \quad \hat{T}_2(\Phi) = \hat{T}_4(\Phi) = \hat{X} \cdot (-\cos \Phi) + \hat{Y} \cdot (\sin \Phi) + \\ \hat{Z} \cdot [(-\zeta_T) \cdot (\cos \Phi_T) \cdot (\sin \Phi) + (\zeta_T) \cdot (\sin \Phi_T) \cdot (-1 + \cos \Phi)].$$

Computing the tilt angles to first order, using the equations of Table 2 gives:

$$(C.08) \quad \tau_{xe}(\Phi) = [(\zeta_T) \cdot (\cos \Phi_T) \cdot (-1 + \cos \Phi) + (\zeta_T) \cdot (\sin \Phi_T) \cdot (\sin \Phi)].$$

$$(C.09) \quad \tau_{ye}(\Phi) = [(-\zeta_T) \cdot (\cos \Phi_T) \cdot (\sin \Phi) + (\zeta_T) \cdot (\sin \Phi_T) \cdot (-1 + \cos \Phi)].$$

The tiltmeter measurement data is least-squares-fitted to (C.08) to obtain the track parameters.

Appendix D. Range Measurements Of Alidade Structure Targets

Pointing coefficient information may be derived by measuring trajectories of alidade-mounted retroreflectors as the telescope rotates in azimuth. In 1999, four ball retroreflector targets will be mounted underneath the elevation bearing support weldments located at each end of the alidade. Distance measurements will subsequently be made from laser rangefinders around the telescope base to those targets. For any alidade azimuth, at least two lines of sight will be available on the right side of the alidade and two more on the left side, towards the bottom surface of each weldment. The midpoint of the line between the right and left side ball centers at each of the alidade ends defines a line which can be used to find the elevation axis of the telescope, independent of the tipping structure's elevation. In the alidade frame of reference this line is at a constant offset from the elevation axis. After the elevation axis direction has been determined at some reference telescope position (by tracking orbit planes of tipping structure targets and finding the common normal to this plane) and this sub-bearing line has been determined at the same telescope reference position, the constant vertical and horizontal offset angles between this line and the elevation axis become available. One may then track the direction of the elevation axis by observations of the sub-bearing targets using the ground rangefinders, without having to vary the telescope in elevation. It is expected that the horizontal angle of the sub-bearing line could be measured to 1 arc-second, and the vertical tilt of this line to 2 arc-second, and the accuracy of the elevation axis would be determined to the same accuracy.

Observations of the direction of this sub-bearing line can be used to correct for non-linearity of the azimuth encoder and obtain corrections for track-nonuniformity. The measurement procedure is analogous to that used for the tiltmeters. Using ground rangefinders, the direction of the sub-bearing reference line is measured versus azimuth encoder readout angle. It is then possible to derive from the measurement results the track rotation angle, Φ , versus the azimuth encoder readout angle, AZ_{enc} . (By definition $\Phi = 0$ when $AZ_{\text{enc}} = 0$).

Let the unit vector pointing along the sub-bearing reference line(Fig. 2) be \hat{U}_{sb} . This line is rigidly tied to the elevation axis to the extent that the bearing platforms are rigidly related to one another. We may write its coordinates as

$$(D.01) \quad \hat{U}_{sb}(\Phi) = \sqrt{1 - \gamma_{sb}^2 - \beta_{sb}^2} \cdot \hat{X}_a(\Phi) + (\gamma_{sb}) \cdot \hat{Y}_a(\Phi) + (-\beta_{sb}) \cdot \hat{W}.$$

When the alidade is at uniform temperature, the small parameters γ_{sb} and β_{sb} are constants. Basis vectors $\hat{X}_a(\Phi)$, $\hat{Y}_a(\Phi)$, and \hat{W} are defined by equations (B.11).

We note that, to first order,

$$(D.02) \quad \hat{X}_r(\Phi) = \hat{U}_{sb}(\Phi) + (\gamma_{el} - \gamma_{sb}) \cdot \hat{Y}_a(\Phi) + (\beta_{sb} - \beta_{el}) \cdot \hat{W}.$$

Parameters γ_{sb} and β_{sb} are obtained by trilateration ranging of the centers of the four sub-bearing balls when the telescope is at standard position, with $AZ_{\text{enc}} = 0$. The coordinates of the midpoint between the centers of the balls under each bearing platform are computed using measured ball center coordinates. The unit direction vector along the line of centers is then computed, to give γ_{sb} and β_{sb} .

After these parameters have been obtained, one computes a table of the ground frame \hat{Y} -component of vector $\hat{U}_{sb}(\Phi)$ versus Φ using equations (D.01) and either (B.11) or (B.12). For each measured value of $\hat{U}_{sb}(AZ_{\text{enc}}) \cdot \hat{Y}$ one looks up the corresponding value of Φ . This provides us with a correction table of the measured track rotation angle Φ versus the azimuth encoder readout angle AZ_{enc} . The function $\Phi(AZ_{\text{enc}})$ is then Fourier analyzed to give $d_{1,1}^{(AZ)}$ and $c_{1,1}^{(AZ)}$.

Appendix E. Computation Of First Order Corrections.

Computation of pointing coefficients to first order involves much algebraic manipulation. To do the computations one needs efficient notation. Telescope small angle parameters are sufficiently small that one can simplify; they are considered to be “first order quantities.” Rules of computation for first order quantities are used.

Let u and v be first order quantities. We assume the following rules:

- (FO-1) $u^2 = 0, \quad v^2 = 0, \quad uv = 0.$
- (FO-2) $\sin u = u, \quad \cos u = 1.$
- (FO-3) $\cos(M + u) = \cos M - u \cdot \sin M,$
- (FO-4) $\sin(M + u) = \sin M + u \cdot \cos M.$

The following quantities appear in the mechanical pointing series computations:

Ω	Alidade rotation angle,
AZ_{com}	Commanded Azimuth,
EL_{com}	Commanded Elevation,
EL_{rig}	GBT Rigging Angle,
$EL_{grav}(EL_{com})$	Gravity elevation shift,
A_0	Paraboloid axis' Azimuth Offset at standard position,
E_0	Paraboloid axis' Elevation Offset at standard position,
ζ_T	GBT zenith angle,
Φ_T	Alidade track azimuth parameter,
β_{el}	Elevation axis angle excess from perpendicularity to azimuth axis,
γ_{el}	Elevation axis' horizontal azimuth offset from \widehat{X} direction is $(-\gamma_{el})$,
ρ_s, ρ_c	Parameters generating EL_{grav} (cf equation B.27).

To simplify the computations we use abbreviated notation:

$$\begin{array}{llll}
M & = & EL_{com} & \zeta_{TX} & = & \zeta_T \cdot \sin \Phi_T \\
S_M & = & \sin EL_{com} & \zeta_{TY} & = & \zeta_T \cdot \cos \Phi_T \\
C_M & = & \cos EL_{com} & \alpha & = & \beta_{el} + \zeta_T \cdot \sin \Phi_T \\
S_{2M} & = & \sin(2 \cdot EL_{com}) & \kappa & = & A_0 + \gamma_{el} \\
C_{2M} & = & \cos(2 \cdot EL_{com}) & \epsilon & = & E_0 \\
S_{nM} & = & \sin(n \cdot EL_{com}) & C_{nM} & = & \cos(n \cdot EL_{com}) \\
L & = & EL_{rig} & \gamma & = & \gamma_{el} \\
S_L & = & \sin EL_{rig} & C_L & = & \cos EL_{rig} \\
S_{2L} & = & \sin(2 \cdot EL_{rig}) & C_{2L} & = & \cos(2 \cdot EL_{rig}) \\
G(M) & = & EL_{grav}(EL_{com}) & & & \\
\rho_L & = & \rho_c \cdot \cos L + \rho_s \cdot \sin L & \rho_M & = & \rho_c \cdot \cos M + \rho_s \cdot \sin M \\
S_\Omega & = & \sin \Omega & C_\Omega & = & \cos \Omega
\end{array}$$

To get pointing series coefficients we first calculate differences of the Cartesian coordinates of the as-built telescope's paraboloid axis, at the commanded beam angles, from the corresponding coordinates for the ideal design telescope. We then compute the quantities ΔEL and $(\cos EL_{com} \cdot \Delta AZ)$ which appear in equations (4.18) and (4.19). These are sums of harmonic terms in commanded elevation and azimuth. The terms are compared to those in Condon's series' for the same quantities, to get *a-priori* estimates for the pointing coefficients.

We first calculate

$$(E.01a) \quad d P_X = P_X - Q_X = \hat{P} \cdot \hat{X} - C_M \cdot S_\Omega ,$$

$$(E.01b) \quad d P_Y = P_Y - Q_Y = \hat{P} \cdot \hat{Y} - C_M \cdot C_\Omega ,$$

$$(E.01c) \quad d P_Z = P_Z - Q_Z = \hat{P} \cdot \hat{Z} - S_\Omega .$$

Condon's expressions for the pointing series' can be written:

$$(E.02a) \quad \Delta EL = \Delta EL^{refraction} + d_{0,0}^{(EL)} +$$

$$+ \sum_m \sum_n \left\{ \begin{aligned} & a_{m,n}^{(EL)} \cdot S_{m\Omega} \cdot S_{nM} + b_{m,n}^{(EL)} \cdot C_{m\Omega} \cdot S_{nM} + \\ & c_{m,n}^{(EL)} \cdot S_{m\Omega} \cdot C_{nM} + d_{m,n}^{(EL)} \cdot C_{m\Omega} \cdot C_{nM} \end{aligned} \right\}.$$

$$(E.02b) \quad EL_{com} \cdot \Delta AZ = d_{0,0}^{(AZ)} + \sum_m \sum_n \left\{ \begin{aligned} & a_{m,n}^{(AZ)} \cdot S_{m\Omega} \cdot S_{nM} + b_{m,n}^{(AZ)} \cdot C_{m\Omega} \cdot S_{nM} + \\ & c_{m,n}^{(AZ)} \cdot S_{m\Omega} \cdot C_{nM} + d_{m,n}^{(AZ)} \cdot C_{m\Omega} \cdot C_{nM} \end{aligned} \right\},$$

where all indexed quantities **a**, **b**, **c**, **d** are independent of Ω and M .

The Cartesian coordinates of \hat{P}_0 are:

$$(E.03a) \quad P_{0X} = (\sin A_0) \cdot \cos(EL_{rig} + E_0),$$

$$(E.03b) \quad P_{0Y} = (\cos A_0) \cdot \cos(EL_{rig} + E_0),$$

$$(E.03c) \quad P_{0Z} = \sin(EL_{rig} + E_0).$$

Expanding the trigonometric sum terms, carrying terms only to first order, and introducing the abbreviated notation, we obtain a first order expression for \hat{P}_0 ,

$$(E.04) \quad \hat{P}_0 = \hat{X} \cdot (A_0 \cdot C_L) + \hat{Y} \cdot (C_L - \epsilon \cdot S_L) + \hat{Z} \cdot (S_L + \epsilon \cdot C_L).$$

We carry out computations to first order. We first carry out a right hand rotation of \hat{P}_0 about the axis

$$(E.05) \quad \hat{X}_r(\Phi = 0) = \hat{X}_{r0} = \hat{X} \cdot (1) + \hat{Y} \cdot (\gamma) + \hat{Z} \cdot (-\alpha) \quad \text{by the angle }.$$

$$(E.06) \quad EL_{com} + EL_{grav} - EL_{rig} = M + G - L \quad \text{to give}$$

$$(E.07) \quad \hat{P}_1 = \hat{X}_{r0} [\hat{X}_{r0} \cdot \hat{P}_0] + [\hat{P}_0 - \hat{X}_{r0} (\hat{X}_{r0} \cdot \hat{P}_0)] \cdot \cos(M + G - L) + \\ + [\hat{X}_{r0} \times \hat{P}_0] \cdot \sin(M + G - L).$$

We then carry out a left hand rotation about telescope zenith \widehat{W} by the azimuth track rotation angle Ω , to give

$$(E.08) \quad \widehat{P} = \widehat{W} \left[\widehat{W} \cdot \widehat{P}_1 \right] \cdot (1 - \cos \Omega) + \widehat{P}_1 (\cos \Omega) + \left[\widehat{P}_1 \times \widehat{W} \right] \cdot (\sin \Omega).$$

After extensive manipulation and reduction we get, to first order:

$$(E.09) \quad \begin{aligned} \widehat{P}_1 = & \widehat{X} \cdot [\kappa \cdot C_L - \alpha \cdot S_L - \gamma \cdot C_M + \alpha \cdot S_M] \\ & + \widehat{Y} \cdot [C_M - \epsilon \cdot S_M - G \cdot S_M] \\ & + \widehat{Z} \cdot [S_M + \epsilon \cdot C_M + G \cdot C_M] . \end{aligned}$$

Using the first order value

$$(E.10) \quad \widehat{W} = \widehat{X} \cdot (\zeta_{TX}) + \widehat{Y} \cdot (\zeta_{TY}) + \widehat{Z} \cdot (1)$$

we carry out rotation (E.08). After some reduction we get, to first order:

$$(E.11) \quad \widehat{P} =$$

$$\begin{aligned} & \widehat{X} \cdot \left[\begin{array}{l} C_M \cdot S_\Omega + (\kappa \cdot C_L - \alpha \cdot S_L) \cdot C_\Omega + (\zeta_{TX}) \cdot S_M \\ -(\epsilon + \zeta_{TY}) \cdot S_M \cdot S_\Omega + (\alpha - \zeta_{TX}) \cdot S_M \cdot C_\Omega \\ +(-\gamma) \cdot C_M \cdot C_\Omega - G \cdot S_M \cdot S_\Omega \end{array} \right] \\ & + \widehat{Y} \cdot \left[\begin{array}{l} C_M \cdot C_\Omega + (\alpha \cdot S_L - \kappa \cdot C_L) \cdot S_\Omega + (\zeta_{TY}) \cdot S_M \\ +(\zeta_{TX} - \alpha) \cdot S_M \cdot S_\Omega + (\gamma) \cdot C_M \cdot S_\Omega \\ -G \cdot S_M \cdot C_\Omega - (\epsilon + \zeta_{TY}) \cdot S_M \cdot C_\Omega \end{array} \right] \\ & + \widehat{Z} \cdot \left[\begin{array}{l} S_M + (\zeta_{TY} + \epsilon) \cdot C_M + G \cdot C_M \\ +(-\zeta_{TX}) \cdot C_M \cdot S_\Omega + (-\zeta_{TY}) \cdot C_M \cdot C_\Omega \end{array} \right] \quad \text{where} \end{aligned}$$

$$(E.12) \quad G = (-\rho_c \cdot C_L - \rho_s \cdot S_L) + \rho_c \cdot C_M + \rho_s \cdot S_M .$$

Using this result in (E.01) gives

$$(E.13) \quad dP_Z = dEL \cdot C_M = -\Delta EL \cdot C_M =$$

$$(\zeta_{TY} + \epsilon) \cdot C_M + (-\rho_c \cdot C_L - \rho_s \cdot S_L) \cdot C_M + \rho_c \cdot C_M \cdot C_M$$

$$+ \rho_s \cdot S_M \cdot C_M + (-\zeta_{TX}) \cdot C_M \cdot S_\Omega + (-\zeta_{TY}) \cdot C_M \cdot C_\Omega .$$

$$(E.14) \quad dP_X =$$

$$(\zeta_{TX}) \cdot S_M + (\kappa \cdot C_L - \alpha \cdot S_L) \cdot C_\Omega - (\epsilon + \zeta_{TY}) \cdot S_M \cdot S_\Omega$$

$$+ (\alpha - \zeta_{TX}) \cdot S_M \cdot C_\Omega + (\rho_c \cdot C_L + \rho_s \cdot S_L) \cdot S_M \cdot S_\Omega$$

$$+ (-\rho_c) \cdot C_M \cdot S_M \cdot S_\Omega + (-\rho_s) \cdot S_M \cdot S_M \cdot S_\Omega + (-\gamma) \cdot C_M \cdot C_\Omega .$$

Substituting (E.13) and (E.14) into (4.17) and (4.19) and combining terms gives:

$$(E.15) \quad (C_M) \cdot \Delta AZ = -(C_M) \cdot dAZ =$$

$$= -(C_\Omega)^{-1} \cdot dP_X - (C_\Omega)^{-1} \cdot (S_\Omega) \cdot (C_M)^{-1} \cdot (S_M) \cdot dP_Z =$$

$$(-\kappa \cdot C_L + \alpha \cdot S_L) + (\zeta_{TX} - \alpha) \cdot S_M + (\gamma) \cdot C_M + (-\zeta_{TX}) \cdot S_M \cdot C_\Omega + (\zeta_{TY}) \cdot S_M \cdot S_\Omega .$$

The azimuth pointing series then becomes

$$(E.16) \quad (C_M) \cdot \Delta AZ =$$

$$[(-A_0 - \gamma_{el}) \cdot \cos EL_{rig} + (\beta_{el} + \zeta_{TX}) \cdot \sin EL_{rig}] + (\gamma_{el}) \cdot C_M +$$

$$+ (-\beta_{el}) \cdot S_M + (-\zeta_{TX}) \cdot C_\Omega \cdot S_M + (\zeta_{TY}) \cdot S_\Omega \cdot S_M .$$

The elevation pointing series then becomes

$$\begin{aligned}
 \text{(E.17)} \quad \Delta EL = & \\
 & [(-E_0 - \zeta_{TY}) + \rho_c \cdot \cos EL_{rig} + \rho_s \cdot \sin EL_{rig}] + (\zeta_{TX}) \cdot S_\Omega + \\
 & + (\zeta_{TY}) \cdot C_\Omega + (-\rho_c) \cdot C_M + (-\rho_s) \cdot S_M .
 \end{aligned}$$

Term-by-term comparison of the components of the above series with those of Condon's series then gives the coefficients listed in Table 1b.

Appendix F. Astronomical To Geodetic Correction.

The pointing coefficients given earlier are used to correct the commanded beam position angles relative to an astronomical local horizon system, that is where the \hat{Z} direction is the local sky zenith, the \hat{Y} direction is locally horizontal and has no eastward component and the \hat{X} , \hat{Y} , and \hat{Z} , directions are mutually perpendicular.

Radio sky-object coordinates are given in a “star-fixed” equatorial system. Coordinates of the radio object in this system are tabulated declination and right ascension at a given epoch. These must be converted to topographic horizon coordinates. To accomplish this, coordinates of the object are converted to geodetic horizon coordinates corresponding to (geodetic) latitude and longitude of the origin of the local topographic system. The resulting geodetic coordinates include corrections for precession and nutation of the rotation axis of the earth, and also refraction. (Geodetic coordinates are referenced to a standard rotational ellipsoidal model of the earth. The available latitude and longitude for the GBT are referenced to the North American datum NAD83.)

Commanded encoder elevation and azimuth angles given relative to the astronomical horizon system (computed using pointing series without any astronomical-to-geodetic coordinate system transformation) must then be additionally corrected to take account of the difference in spatial orientation of the local astronomical and geodetic frames. This correction is time-independent.

A service for performing these computations is provided by the National Geodetic Survey of the NOAA. This service is available on the Internet at address “http://www.ngs.noaa.gov/DEFLEC/deflec_comp.html”. Geodetic latitude and longitude of the local coordinate system’s origin are supplied by the user. The program “DEFLEC96” returns three angles: Xi Deflec. (arc seconds), Eta Deflec. (arc seconds), and Hor. Laplace (arc seconds). The sign conventions used and definitions of these quantities are also returned. Given the three quantities, the astronomical to geodetic azimuth and elevation corrections can be computed.

Available NAD83 survey values (deg min sec) were entered for GBT Station location:

$$(F.01) \quad LAT(N) = 38\ 25\ 59.23658, \quad LONG(W) = 79\ 50\ 23.4054.$$

The DEFLEC 96 program returned

$$(F.02) \quad \xi = -3.43, \quad \eta = 1.33, \quad Hor. Laplace = -1.06 \text{ (arc sec)}.$$

Converting these angle components to radians we use:

$$(F.04) \quad \xi = -16.6 \times 10^{-6}, \quad \eta = +6.45 \times 10^{-6} \text{ (radian)}.$$

Quantities ξ and η are defined as follows (Fig. 7). Let λ be geodetic longitude and ϕ geodetic latitude at the GBT track-top center. Let Λ be astronomical longitude and Φ be astronomical latitude at the same point. Then,

$$(F.05) \quad \xi = \Phi - \phi, \quad \eta = (\Lambda - \lambda) \cdot \cos \phi.$$

Quantity ξ is the deflection of the vertical along the meridian, η is the deflection of the vertical along the prime vertical.

The geodetic latitude and longitude of the GBT track-top center are:

$$(F.06) \quad \phi = +38\ 25\ 59.23658, \quad \lambda = -79\ 50\ 23.4054 \text{ (d m s)}.$$

Definitions of these quantities are given and discussed in [Coo 87].

Computation of geodetic pointing corrections proceeds as follows. We assume that the commanded beam angles given to the telescope are to be corrected so that the telescope paraboloid's axis points to geodetic azimuth Ω and geodetic elevation M . The commanded beam azimuth and elevation angles to be given to the GBT drive motors are thereby assumed to be $\Omega + \Delta\Omega$ and $M + \Delta M$ respectively. As before, we let \hat{P} be a unit vector in the direction in which the paraboloid axis is to point. Let \hat{H}_E be the direction of the normal, to the earth reference ellipsoid, which passes through the track-top center of the GBT. Let \hat{N} be the direction of

geodetic North and \widehat{E} be the direction of geodetic East at this point.

We desire that the telescope should point in the direction:

$$(F.07) \quad \widehat{P} = (C_M \cdot S_\Omega) \cdot \widehat{E} + (C_M \cdot C_\Omega) \cdot \widehat{N} + (S_M) \cdot \widehat{H}_E .$$

To achieve this we demand that the telescope paraboloid axis be brought to the attitude

$$(F.08) \quad \widehat{P} = (C_{M+\Delta M} \cdot S_{\Omega+\Delta\Omega}) \cdot \widehat{X} + (C_{M+\Delta M} \cdot C_{\Omega+\Delta\Omega}) \cdot \widehat{Y} + (S_{M+\Delta M}) \cdot \widehat{Z} .$$

Geodetic and astronomical coordinate frames are related, to first order by the relation:

$$(F.09) \quad \begin{bmatrix} \widehat{E} \\ \widehat{N} \\ \widehat{H}_E \end{bmatrix} = \begin{bmatrix} 1 & -\eta \cdot \tan \phi & \eta \\ \eta \cdot \tan \phi & 1 & \xi \\ -\eta & -\xi & 1 \end{bmatrix} \cdot \begin{bmatrix} \widehat{X} \\ \widehat{Y} \\ \widehat{Z} \end{bmatrix} .$$

To show this we use the defining equations for these frames. Those frames are defined with respect to an earth reference ellipsoid centered frame: $\widehat{I}, \widehat{J}, \widehat{K}$. The ellipsoid unit basis vector \widehat{I} is directed from the ellipsoid center along longitude -90° , latitude 0° ; \widehat{J} is directed from the ellipsoid center along longitude 0° , latitude 0° and \widehat{K} is directed along the ellipsoid minor axis. The geometry is shown in Figure 7. The defining equations of the geodetic and astronomical reference frame unit basis vectors are then:

$$\begin{aligned}
\widehat{H}_E &= \widehat{I}(-C_\phi \cdot S_\lambda) + \widehat{J}(C_\phi \cdot C_\lambda) + \widehat{K}(S_\phi) , \\
\widehat{N} &= \widehat{I}(-C_{\phi+90^\circ} \cdot S_\lambda) + \widehat{J}(C_{\phi+90^\circ} \cdot C_\lambda) + \widehat{K}(S_{\phi+90^\circ}) , \\
&= \widehat{I}(S_\phi \cdot S_\lambda) + \widehat{J}(-S_\phi \cdot C_\lambda) + \widehat{K}(C_\phi) , \\
\widehat{E} &= \widehat{N} \times \widehat{H}_E = \widehat{I} \cdot (-C_\lambda) + \widehat{J} \cdot (-S_\lambda) , \\
\widehat{Z} &= \widehat{I}(-C_\Phi \cdot S_\Lambda) + \widehat{J}(C_\Phi \cdot C_\Lambda) + \widehat{K}(S_\Phi) , \\
\widehat{Y} &= \widehat{I}(-C_{\Phi+90^\circ} \cdot S_\Lambda) + \widehat{J}(C_{\Phi+90^\circ} \cdot C_\Lambda) + \widehat{K}(S_{\Phi+90^\circ}) , \\
&= \widehat{I}(S_\Phi \cdot S_\Lambda) + \widehat{J}(-S_\Phi \cdot C_\Lambda) + \widehat{K}(C_\Phi) , \\
\widehat{X} &= \widehat{Y} \times \widehat{Z} = \widehat{I} \cdot (-C_\Lambda) + \widehat{J} \cdot (-S_\Lambda) .
\end{aligned}
\tag{F.10}$$

By definition:

$$(F.11) \quad \eta = (\Lambda - \lambda) \cdot C_\phi , \quad \xi = \Phi - \phi , \quad \text{which gives}$$

$$(F.11.i) \quad \Lambda = \lambda + \eta \cdot C_\phi^{-1} , \quad \Phi = \phi + \xi .$$

For small $\eta, \xi, n \cdot C_\phi^{-1}$, the trigonometric angle sum formulas give:

$$\begin{aligned}
S_\Lambda &= S_\lambda + \eta \cdot C_\phi^{-1} \cdot C_\lambda , \\
C_\Lambda &= C_\lambda - \eta \cdot C_\phi^{-1} \cdot S_\lambda , \\
S_\Phi &= S_\phi + \xi \cdot C_\phi , \\
C_\Phi &= C_\phi - \xi \cdot S_\phi .
\end{aligned}
\tag{F.12}$$

Inverting the first three equations of (F.10) gives

$$(F.13)$$

$$\begin{aligned}
\widehat{I} &= \widehat{E} \cdot (-C_\lambda) + \widehat{N} \cdot (S_\phi \cdot S_\lambda) + \widehat{H}_E \cdot (-C_\phi \cdot S_\lambda) , \\
\widehat{J} &= \widehat{E} \cdot (-S_\lambda) + \widehat{N} \cdot (-S_\phi \cdot C_\lambda) + \widehat{H}_E \cdot (C_\phi \cdot C_\lambda) , \\
\widehat{K} &= \widehat{N} \cdot (C_\phi) + \widehat{H}_E \cdot (S_\phi) .
\end{aligned}$$

Substituting relations (F.12) into the last three equations of (F.10), and retaining terms to first order gives

(F.14)

$$\begin{aligned}
\widehat{X} &= \widehat{I}(-C_\lambda + \eta \cdot C_\phi^{-1} \cdot S_\lambda) + \widehat{J}(-S_\lambda - \eta \cdot C_\phi^{-1} \cdot C_\lambda) , \\
\widehat{Y} &= \widehat{I} \cdot (S_\phi \cdot S_\lambda + \xi \cdot C_\phi \cdot S_\lambda + \eta \cdot \tan \phi \cdot C_\lambda) \\
&\quad + \widehat{J} \cdot (-S_\phi \cdot C_\lambda - \xi \cdot C_\phi \cdot C_\lambda + \eta \cdot \tan \phi \cdot S_\lambda) + \widehat{K} \cdot (C_\phi - \xi \cdot S_\phi) , \\
\widehat{Z} &= \widehat{I} \cdot (-C_\phi \cdot S_\lambda + \xi \cdot S_\phi \cdot S_\lambda - \eta \cdot C_\lambda) \\
&\quad + \widehat{J} \cdot (C_\phi \cdot C_\lambda - \xi \cdot S_\phi \cdot C_\lambda - \eta \cdot S_\lambda) + \widehat{K} \cdot (S_\phi + \xi \cdot C_\phi) .
\end{aligned}$$

Substituting relations (F.13) into (F.14) gives, to first order, the astronomic frame basis vectors in terms of the geodetic frame basis vectors,

(F.15)

$$\begin{aligned}
\widehat{X} &= \widehat{E} + (\eta \cdot \tan \phi) \cdot \widehat{N} - \eta \cdot \widehat{H}_E , \\
\widehat{Y} &= (-\eta \cdot \tan \phi) \cdot \widehat{E} + \widehat{N} - \xi \cdot \widehat{H}_E , \\
\widehat{Z} &= \eta \cdot \widehat{E} + \xi \cdot \widehat{N} + \widehat{H}_E .
\end{aligned}$$

Inversion of (F.15) gives the geodetic frame base vectors in terms of the astronomical frame basis vectors, which are the desired relations (F.09). Substitute (F.09) into (F.07) to express the geodetic pointing requirement (F.07) in terms of ground frame basis vectors. (The local ground frame is the astronomical frame of reference).

This gives:

$$\begin{aligned}
 \text{(F.07b)} \quad \hat{P} = & (C_M \cdot S_\Omega) \cdot (\hat{X} - \eta \cdot \tan \phi \cdot \hat{Y} + \eta \cdot \hat{Z}) + \\
 & + (C_M \cdot C_\Omega) \cdot (\eta \cdot \tan \phi \cdot \hat{X} + \hat{Y} + \xi \cdot \hat{Z}) + \\
 & + (S_M) \cdot (-\eta \cdot \hat{X} - \xi \cdot \hat{Y} + \hat{Z}) , \quad \text{or}
 \end{aligned}$$

$$\begin{aligned}
 \text{(F.07c)} \quad \hat{P} = & (C_M \cdot S_\Omega + C_M \cdot C_\Omega \cdot \eta \cdot \tan \phi - \eta \cdot S_M) \cdot (\hat{X}) + \\
 & + (C_M \cdot C_\Omega - C_M \cdot S_\Omega \cdot \eta \cdot \tan \phi - \xi \cdot S_M) \cdot (\hat{Y}) + \\
 & + (S_M + \eta \cdot C_M \cdot S_\Omega + \xi \cdot C_M \cdot C_\Omega) \cdot (\hat{Z}) .
 \end{aligned}$$

Expanding the trigonometric angle sum terms of (F.08) gives

$$\begin{aligned}
 \text{(F.08b)} \quad \hat{P} = & \\
 & (C_M \cdot C_{\Delta M} - S_M \cdot S_{\Delta M}) \cdot (S_\Omega \cdot C_{\Delta \Omega} + C_\Omega \cdot S_{\Delta \Omega}) \cdot \hat{X} \\
 & + (C_M \cdot C_{\Delta M} - S_M \cdot S_{\Delta M}) \cdot (C_\Omega \cdot C_{\Delta \Omega} - S_\Omega \cdot S_{\Delta \Omega}) \cdot \hat{Y} \\
 & + (S_M \cdot C_{\Delta M} + C_M \cdot S_{\Delta M}) \cdot \hat{Z} .
 \end{aligned}$$

From first order relations (FO-3), (FO-4), we get

$$\begin{aligned}
(\text{F.08c}) \quad \widehat{P} = & \\
& (C_M - S_M \cdot \Delta M) \cdot (S_\Omega + C_\Omega \cdot \Delta \Omega) \cdot \widehat{X} \\
& + (C_M - S_M \cdot \Delta M) \cdot (C_\Omega - S_\Omega \cdot \Delta \Omega) \cdot \widehat{Y} \\
& + (S_M + C_M \cdot \Delta M) \cdot \widehat{Z} .
\end{aligned}$$

Equating the components of \widehat{Z} in (F.07c) with those of \widehat{Z} in (F.08c) gives, after algebraic reduction:

$$(\text{F.16}) \quad \Delta M = (\eta) \cdot S_\Omega + (\xi) \cdot C_\Omega .$$

Equating components of \widehat{X} in (F.07c) with those of \widehat{X} in (F.08c) gives, after algebraic reduction, and substitution of (F.16):

$$(\text{F.17}) \quad C_M \cdot \Delta \Omega = (\eta \cdot \tan \phi) \cdot C_M + (-\eta) \cdot S_M \cdot C_\Omega + (\xi) \cdot S_M \cdot S_\Omega .$$

The last two equations provide our geodetic pointing corrections. They appear as an additive track correction, together with a constant azimuth shift (the horizontal Laplace term) and give the following increments to the pointing coefficients:

$$\begin{aligned}
& \left(a_{1,1}^{(\text{AZ})} \right)_{\text{geodetic}} = +\xi , \\
& \left(b_{1,1}^{(\text{AZ})} \right)_{\text{geodetic}} = -\eta , \\
(\text{F.18}) \quad & \left(d_{0,1}^{(\text{AZ})} \right)_{\text{geodetic}} = +\eta \cdot \tan \phi , \\
& \left(c_{1,0}^{(\text{EL})} \right)_{\text{geodetic}} = +\eta , \\
& \left(d_{1,0}^{(\text{EL})} \right)_{\text{geodetic}} = +\xi .
\end{aligned}$$

These geodetic contributions are included in the coefficients summarized in Section 6. It is possible to check (F.16) and (F.18) independently by use of equations (6.39) through (6.42) found in Leick [Lei 90].

References

- [Con 92] J. J. Condon, "GBT pointing equations", GBT Memo 75, 1992.
- [Coo 87] M. A.R. Cooper, "Control Surveys In Civil Engineering", Nichols Publishing Company, NY, pp. 31-41, 1987.
- [Gol 97] M. A. Goldman, "GBT coordinates and coordinate transformations", GBT Memo 165, February 15, 1997.
- [HGPP 98] R. Hall, M. A. Goldman, D. H. Parker, and J. M. Payne, "Measurement program for the Green Bank Telescope", GBT Memo 186, 1998.
- [Kav 96] B.F. Kavanagh and S.J.G. Bird, "Surveying Principles and Applications," 4'th Ed., Prentice Hall, Englewood Cliffs NJ, pp. 432-443.
- [Kil 1] R. Kilbrick, L. Robinson, and D. Cowley, "An evaluation of precision tilt-sensors for measuring telescope position," in Telescope Control Systems, P.T. Wallace , ed., Proc. SPIE 2479 pp. 341-352, 1995.
- [Kil 98] R. Kilbrick, L. Robinson, V. Wallace, and D. Cowley, "Tests of a precision tiltmeter system for measuring telescope position," Proc. SPIE 3351 pp. 342-353, 1998.
- [Lei 90] A. Leick, "GPS Satellite Surveying," Wiley, NY, 1990, pp. 185-191.
- [MR 98] P. Matheny, and B. Radcliff, "Hydrostatic level operation," GBT Archive LO472.
- [Mor 97] H. Mortin "Measurements on the GBT," GBT Archive A0082, Oct. 01, 1997.
- [Pel 92] P. Pellissier, "Pellissier model H5 portable hydrostatic level/tiltmeter,"

GBT Memo 116, May 1992.

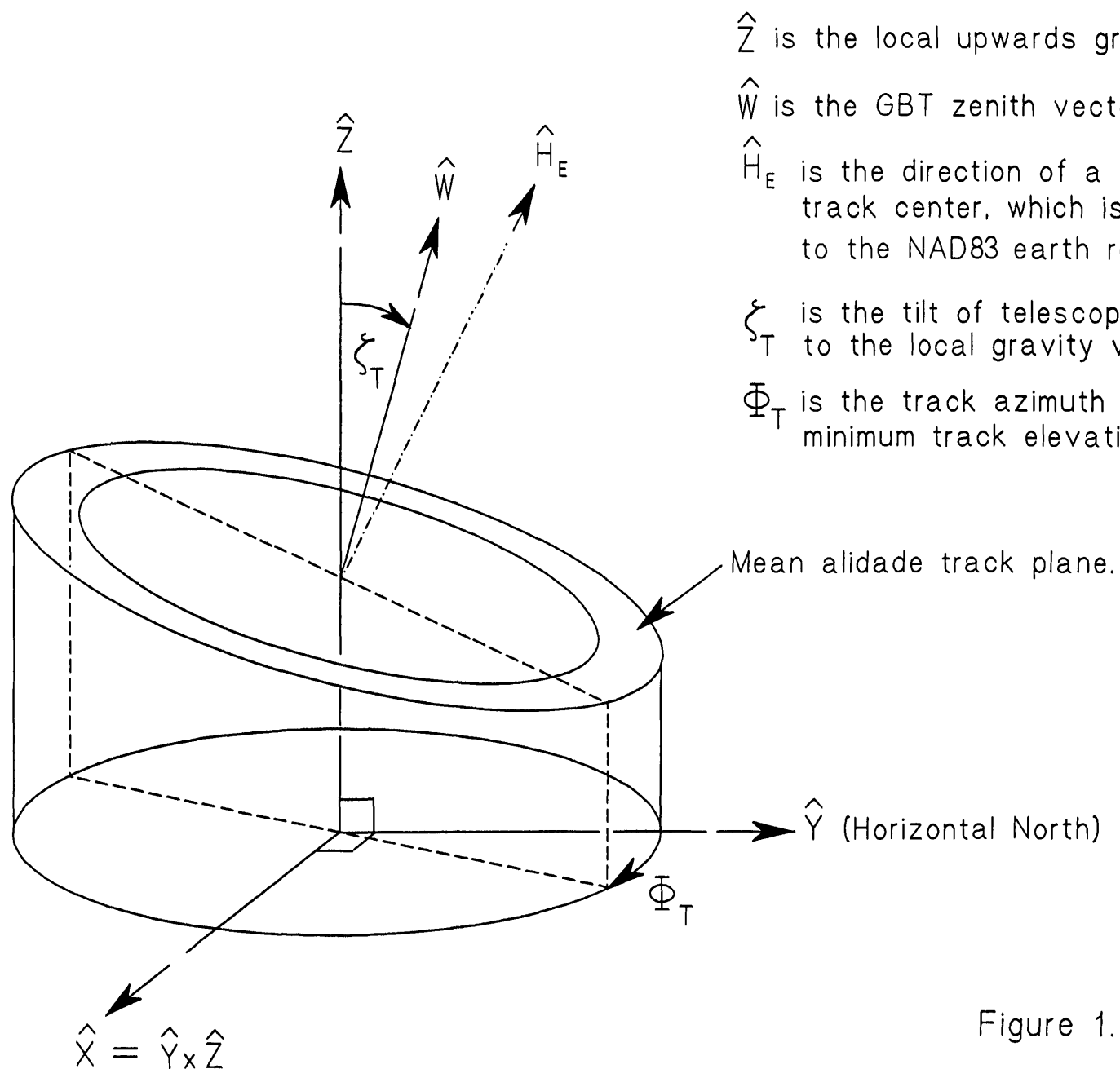
[Pel 93] P. Pellissier, “Benchmarks for accurate leveling,” GBT Memo 117, May 1993.

[Par 97] D.H. Parker, “The Green Bank Telescope Laser Metrology Project, A Review,” GBT Archive LO294, April 1997.

[PG 98] J. M. Payne, and M. A. Goldman, “Proposal for a GBT measurement program”, GBT Memo draft, 1999.

[Wel 95] D. Wells, “The GBT tipping-structure model in C,” GBT Memo 173, January 1998.

[Wel 98] D. Wells, “The Condon series pointing model in C,” GBT Memo 173, January 1998.



\hat{Z} is the local upwards gravity vertical.

\hat{W} is the GBT zenith vector.

\hat{H}_E is the direction of a line, through the track center, which is locally normal to the NAD83 earth reference ellipsoid.

ξ_T is the tilt of telescope zenith to the local gravity vertical.

Φ_T is the track azimuth of minimum track elevation.

Mean alidade track plane.

\hat{Y} (Horizontal North)

Φ_T

$\hat{X} = \hat{Y} \times \hat{Z}$

Figure 1.

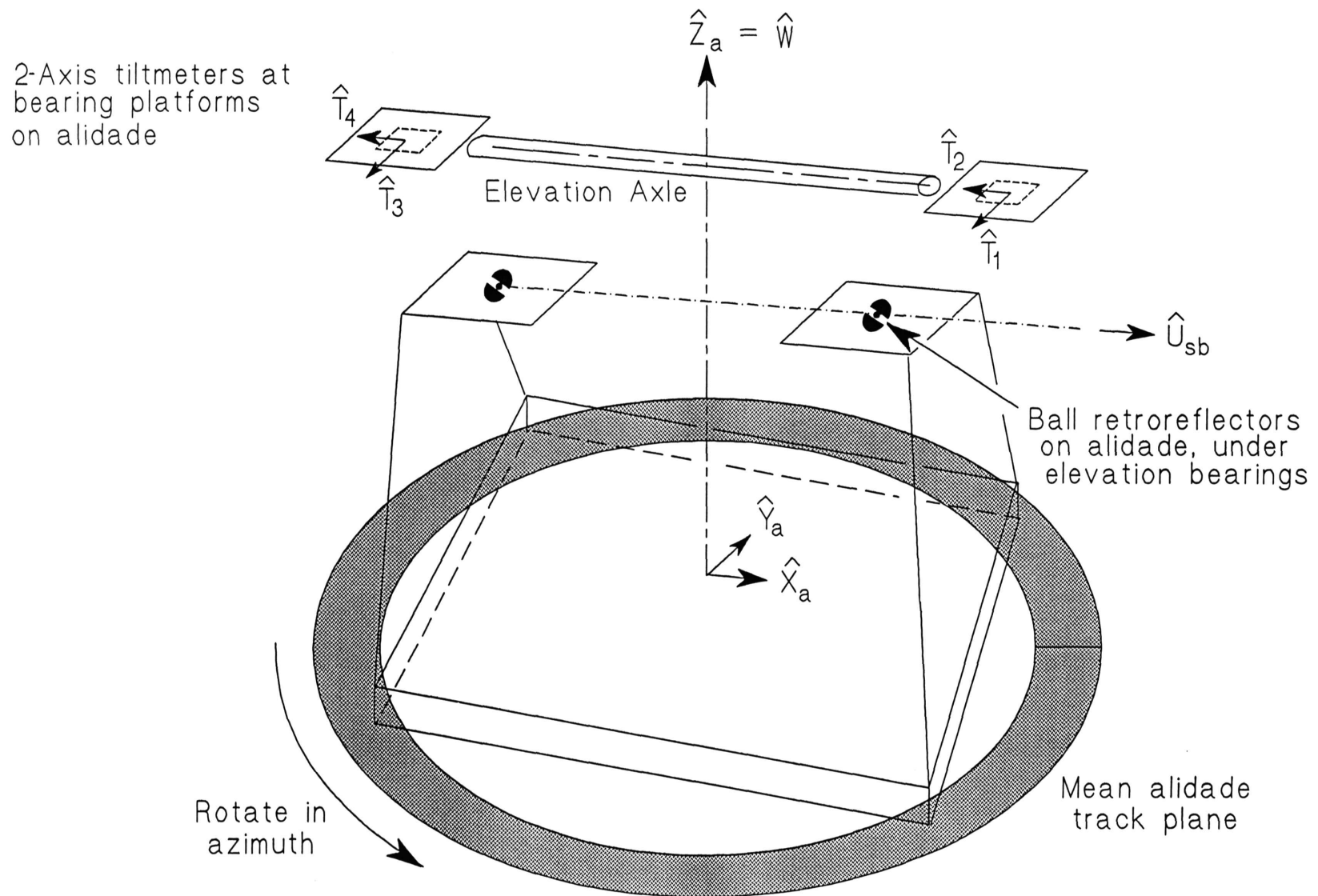


Figure 2.

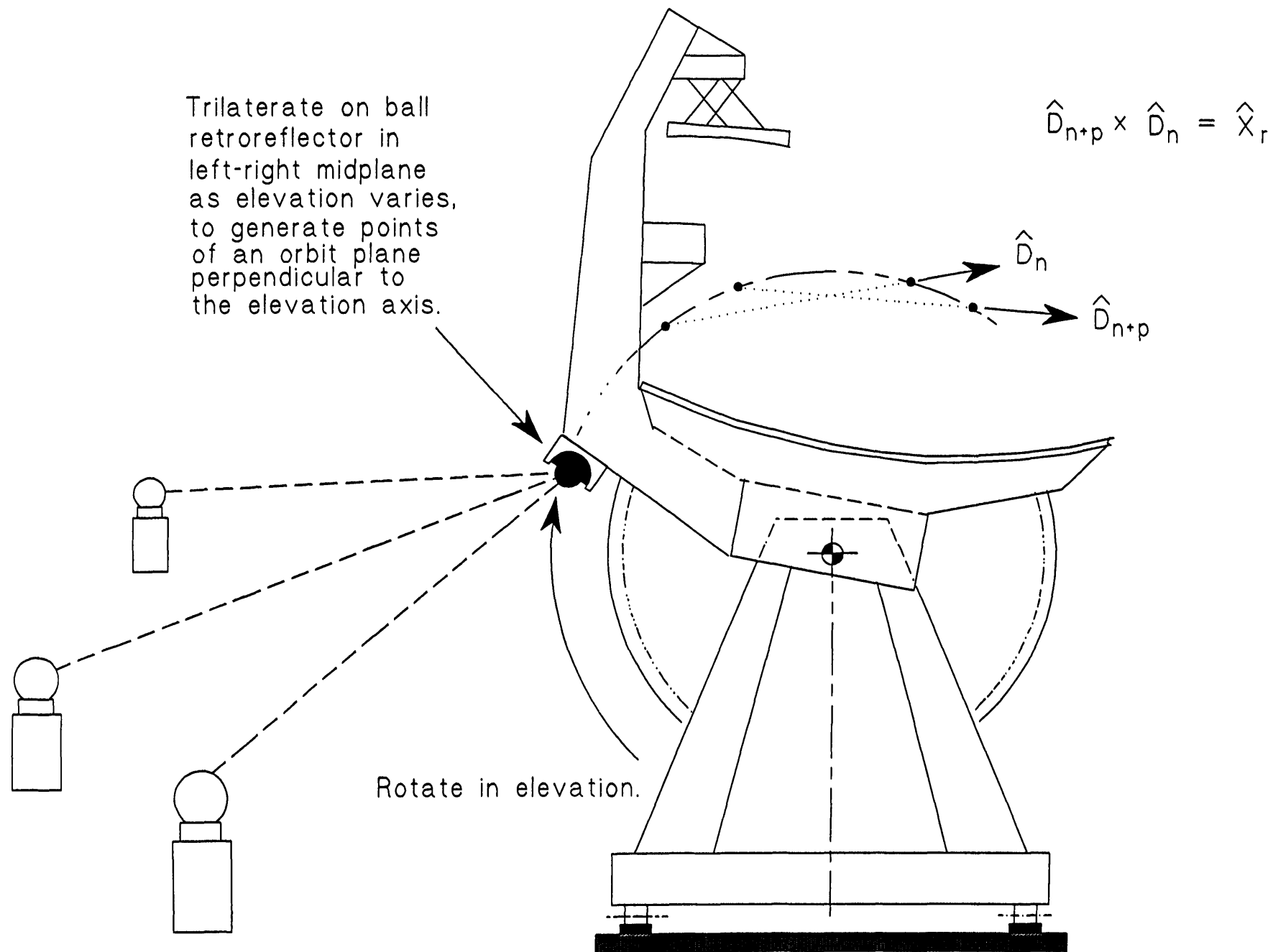


Figure 3. Rangefinder Determination Of The Elevation Axis.

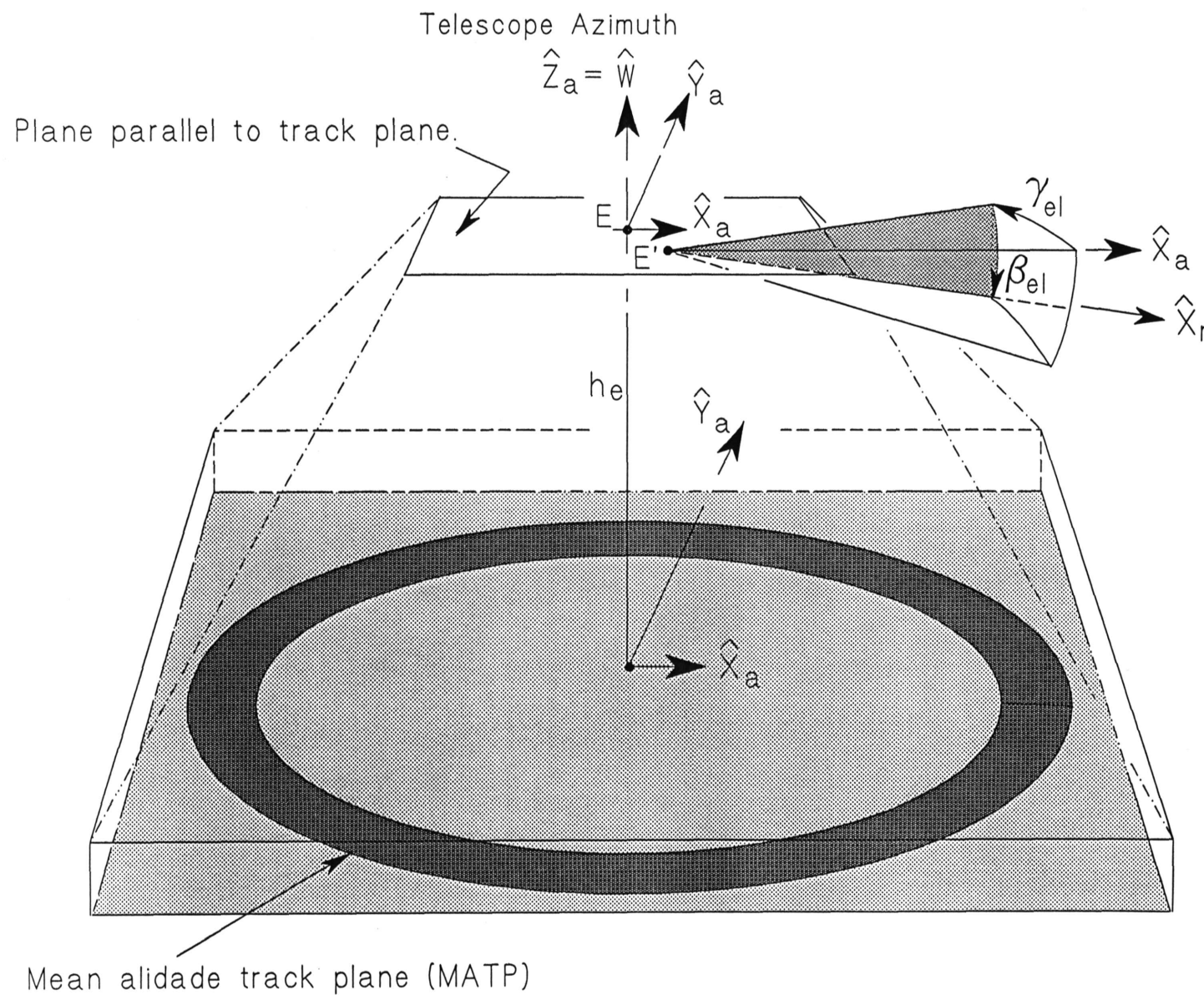
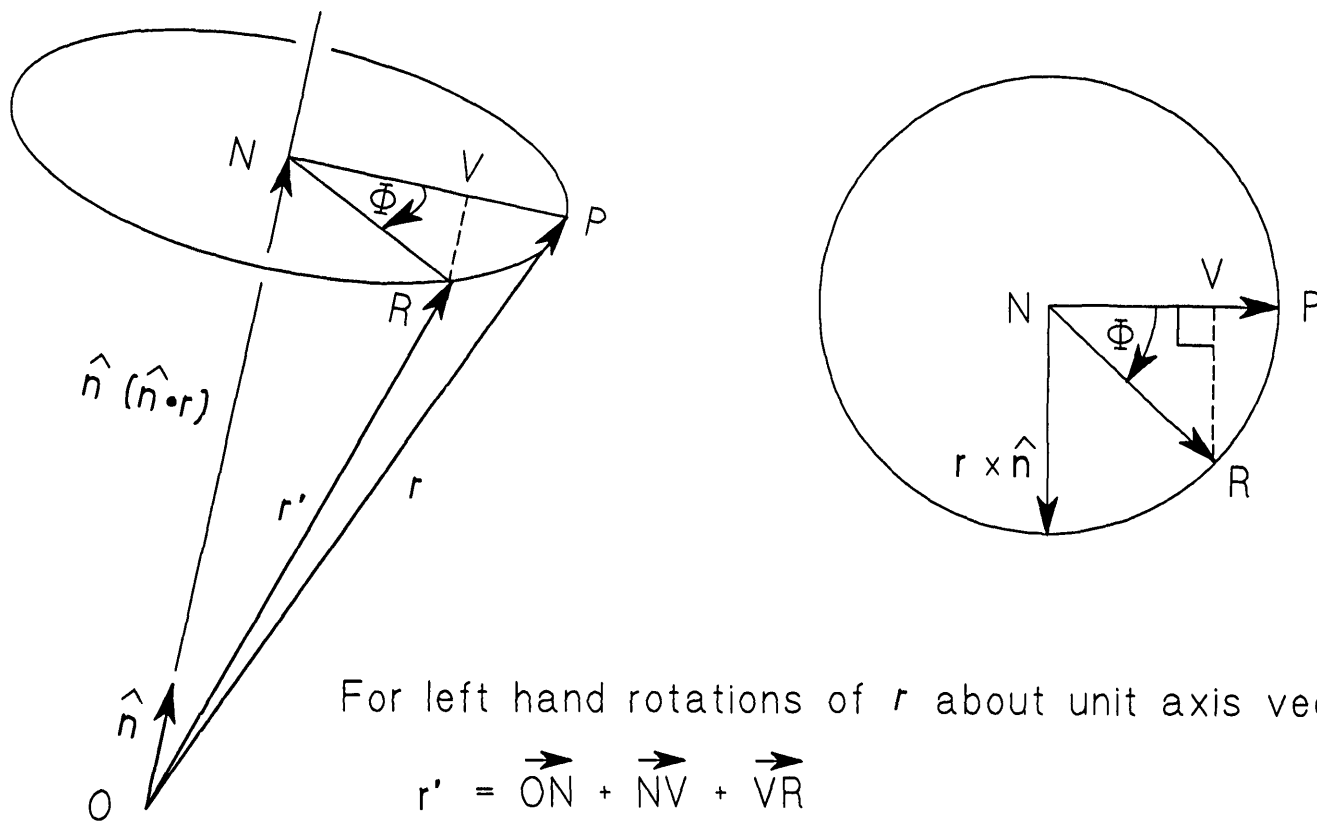


Figure 4. Elevation Axis Offset Geometry



For left hand rotations of r about unit axis vector \hat{n} :

$$r' = \vec{ON} + \vec{NV} + \vec{VR}$$

$$r' = \hat{n} (\hat{n} \cdot r) + [r - \hat{n} (\hat{n} \cdot r)] \cos \Phi + (r \times \hat{n}) \sin \Phi$$

Figure 6. Rotation Of A Vector About An Axis

Table 3. Main Reflector Axis Orientations For Pointing Correction Calculations

Point	Associated Unit Vector	Telescope Encoder Reading	Ground Frame Polar Coordinates
As-Built Telescope			
P_0	\hat{P}_0	$AZ_{enc}(P_0) = 0 \text{ } (= \Phi_0)$ $EL_{enc}(P_0) = EL_{rig}$ ↓ Rotate tipping structure about $\hat{X}_r(\Phi = 0)$ until elevation encoder reads $EL_{enc} = EL_{com}$.	$AZ(P_0) = A_0$ $EL(P_0) = E_0 + EL_{rig}$
P_1	\hat{P}_1	$AZ_{enc}(P_1) = 0, EL_{enc}(P_1) = EL_{com}$ ↓ Rotate alidade structure about telescope zenith direction, \hat{W} , until azimuth encoder reads $AZ_{enc} = AZ_{com} \text{ } (= \Phi)$.	$AZ(P_1), EL(P_1)$
P	\hat{P}	$AZ_{enc}(P) = AZ_{com}$ $EL_{enc}(P) = EL_{com}$	$AZ(P) = AZ_{com} + (-\Delta AZ)$ $EL(P) = EL_{com} + (-\Delta EL)$
Ideal Telescope			
Q_0	\hat{Q}_0	$AZ_{enc}(Q_0) = 0, EL_{enc}(Q_0) = EL_{rig}$ ↓ Rotate tipping structure about \hat{X} until elevation encoder reads EL_{com} .	$AZ(Q_0) = 0, EL(Q_0) = EL_{rig}$
Q_1	\hat{Q}_1	$AZ_{enc}(Q_1) = 0, EL_{enc}(Q_1) = EL_{com}$ ↓ Rotate tipping structure about \hat{Z} until azimuth encoder reads $AZ_{enc} = AZ_{com}$.	$AZ(Q_1) = 0, EL(Q_1) = EL_{com}$
Q	\hat{Q}	$AZ_{enc}(Q) = AZ_{com}$ $EL_{enc}(Q) = EL_{com}$	$AZ(Q) = AZ_{com}$ $EL(Q) = EL_{com}$

Ideal direction vector \hat{Q}_0 points along the design direction of the main reflector surface's optical axis as designed, when azimuth and elevation encoders indicate standard telescope position. Direction vector \hat{P}_0 is assumed to point in the direction of the main reflector surface optical axis, as built and aligned, when the telescope encoders indicate standard position. Parameters A_0 and E_0 are small angle deviations of the as-built paraboloid axis' pointing as set initially (during surface panel alignment), from the ideal values at standard telescope position. The rotations above are computed as functions of track parameters ζ_T and Φ_T , elevation axis parameters β_{el} and γ_{el} , the Finite Element Model calculated gravity deformation elevation correction $EL_{grav}(EL_{com})$, and the rigging elevation angle EL_{rig} , to compute the pointing deviations: $\Delta AZ, \Delta EL$, to be added to the commanded values, in order to direct the (surface-actuator-corrected) paraboloid's axis to polar angles EL_{com}, AZ_{com} with respect to the ground reference frame.

$$\xi = \bar{\Phi} - \phi$$

$$\eta = (\Lambda - \lambda) \cdot \cos \phi$$

$$\phi \text{ (GBT)} = + 38 \ 25 \ 59.23658 \text{ (d m s)}$$

$$\lambda \text{ (GBT)} = - 79 \ 50 \ 23.4054$$

GBT astronomic zenith is the local gravity vertical, \hat{Z} , at the GBT track-top center

GBT geodetic zenith, \hat{H}_E , is the normal to the reference ellipsoid, through the GBT track-top center

ϕ is the geodetic latitude

λ is the geodetic longitude

$\bar{\Phi}$ is the astronomical latitude

Λ is the astronomical longitude

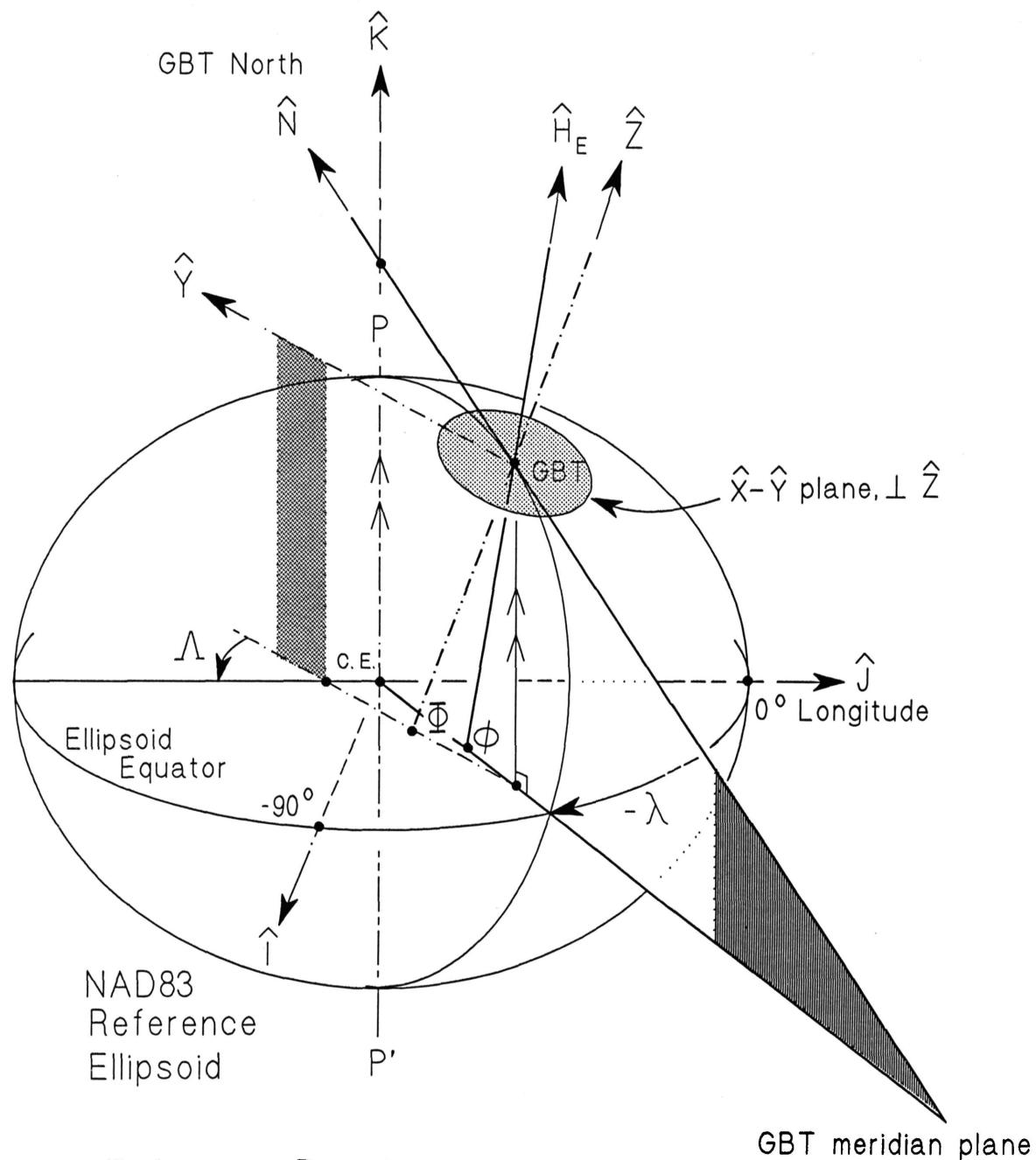


Figure 7. Geodetic And Astronomic Reference Directions.